

CERN-SPSC-2008-013
SPSC-SR-031
15.04.2008

STATUS REPORT OF THE CAST EXPERIMENT

The CAST Collaboration

CEA Saclay -- CERN -- Dogus University -- Lawrence Livermore
National Laboratory --Max-Planck-Institut for Solar System Research/
Katlenberg-Lindau -- Max-Planck-Institut für extraterrestrische
Physik --Max-Planck-Institut für Physik -- National Center for
Scientific Research Demokritos -- NTUA Athens -- Rudjer Boskovic
Institute-- Institute for Nuclear Research (Moscow)-- TU Darmstadt --
University of British Columbia -- University of Chicago --
Universität Frankfurt --Universität Freiburg -- University of Florida --
University of Patras -- University of Thessaloniki -- Universita di
Trieste -- Universidad de Zaragoza -- Universität Zurich



CONTENTS

	Page
1. INTRODUCTION	3
2. SUMMARY SINCE APRIL 2007	3
3. RESULTS FROM ^4He PHASE II	6
3.1 pn-CCD and X-ray mirror system operation	6
3.2 The ^4He sunrise Micromegas analysis	8
3.3 The ^4He TPC detector analysis	10
3.4 Combined results	12
4. DETECTOR STATUS	13
4.1 The CCD Detector Replacement	13
4.2 The new pn-CCD detector and the X-ray telescope	14
4.3 The Bulk and Microbulk Micromegas technology	17
4.4 The Sunrise Micromegas detector	17
4.5 The Sunset Micromegas detectors	19
4.6 The MM line X-ray optics status	21
5. THE ^3He GAS SYSTEM STATUS	23
6. THE VISIBLE MEASUREMENTS AT CAST	30
7. CRYOPLANT STATUS	34
8. THE SLOW CONTROL STATUS	34
9. SUN FILMING	35
10. GRID MEASUREMENTS IN 2008	37
11. CAST EXPERIMENTAL APPARATUS	38
12. PHYSICS JUSTIFICATION	40
13. DETAILS OF RUNNING TIME, COSTS AND RESOURCES REQUIRED FOR 2008 – 2010	41
14. CONCLUSIONS	45

1. INTRODUCTION

The CAST experiment has been designed to search principally for axions of solar origin. The first phase of the experiment (Phase I) explored axion masses up to 0.02 eV and the data taking was successfully completed during 2003 – 2004. Final results from Phase I have been published in JCAP 0704:010, 2007 (hep-ex/0702006) and provide the best experimental limit, to date, on the axion-photon coupling $g_{a\gamma} < 8.8 \times 10^{-11} \text{GeV}^{-1}$ at 95% CL. This limit supersedes or at least competes with the best astrophysical one, deduced from the evolution of the HB stars in globular clusters.

CAST Phase II is extending its research potential to higher axion masses by introducing a buffer gas in the cold bore. ^4He was used as refractive gas during the first period of Phase II to reach masses up to 0.39 eV and the data taking was completed during 2005 – 2006. The scanning required 160 density settings with progressive steps of one pressure setting per day, reaching 13.4 mbar @ 1.8K. The data analysis is finalized and the combined results show that CAST is entering the interesting “axion line” area (Figure 14). During the second period of Phase II CAST can cover masses up to 1.17 eV, using as buffer gas ^3He which presents a saturated vapor pressure of 135 mbar @ 1.8 K. The CAST collaboration’s primary target was to commission a ^3He gas system allowing for a variety of gas operations, fulfilling at the same time the necessary precision and safety requirements against gas loss. The gas system was commissioned by the end of 2007 and it will allow pressure settings up to 120 mbar @ 1.8 K spanning a period of three years. The CAST research potential may extend, for the first time, to the upper HDM axion mass limit. The CAST experiment has recently (end of March 2008) started data taking into this unexplored domain.

In parallel to the main CAST activity, the collaboration extended its search at low energies and performed, for the first time for an axion helioscope, measurements in the visible (axion energy of a few eV) during two periods of one week each. New collaborating institutes participated mainly in this activity affecting only slightly the mainstream CAST program.

The next section gives a summary of the CAST activities since April 2007. We present the finalized analysis of the ^4He run Phase II data for each detector and also the combined result. The following section provides the status of all CAST detectors at the beginning of the ^3He run Phase II data taking period. Then a full description of the ^3He gas system is given. The section that follows describes the measurements at low energies. Next items give the status of the Cryogenics system, the Slow Control, the Sun Filming and the Grid measurements. The last part of the document refers to the CAST experimental apparatus, the Physics justification, manpower, budget estimates, details of Add. No 3 to cover 2008 – 2010, possible scenarios for data taking and the conclusions.

2. SUMMARY SINCE APRIL 2007

We summarize here the milestones that the CAST experiment has achieved since April 2007:

1) ^3He gas system commissioned. This system is an indispensable part of CAST for PHASE II. The initial planning was to have the system ready by the middle of August 2007. The system was finally ready and was commissioned with ^4He in November 2007. Delays were caused by: 1) An error in the engineering drawing of the cryo pipe system near the cold bores,

required readapting the initial drawings and work, 2) late delivery (up to two months) of crucial parts, 3) change of manufacturers due to inadequate material, 4) Due to the LHC commissioning CAST was assigned low priority for mechanical electrical and cryogenic support, 5) baking out of ^4He from the cold bores to avoid ^3He contamination and 6) Some problems occurred in the operation of the mass flow controllers, damaging the electronic cards which had to be sent to the producer for repair. The system is now operational and fulfills all the requirements for precision and safety against gas loss. CAST is taking data with ^3He since the end of March 2008.

2) pn-CCD and X-ray telescope refurbished. Even though, an intervention on the X-ray telescope was not planned, the CCD showed a degraded performance in August 2007. Many saturated, extremely noisy pixels and channels turned the CCD unusable. This effect was caused by metal particle contamination of the CCD chip, originating from the mechanism moving the ^{55}Fe calibration source inside the X-ray telescopes vacuum vessel. A new pn-CCD chip, of the same type, replaced the faulty one, and it restored the performance at the same level as previously. At the same time, the mirror of the X-ray telescope was checked and was measured to have no loss of reflectivity after the four years operation in CAST. The last check required the X-ray telescope dismounting and testing at the PANTER X-ray facility in Munich which was done in parallel to the detector activities. The re-calibration of the X-ray telescope was necessary, to exclude any loss in efficiency due to potential surface contamination, facing the forthcoming three years CAST data taking. The CCD and the X-ray telescope are now fully operational and taking data for the ^3He run Phase II.

3) TPC and Micromegas detectors replacement. The micromegas technology has become mature during the last years and enough experience has been acquired using it with the CAST experiment. In June 2007 the collaboration approved the proposal of the TPC and the micromegas group to replace the sunset TPC detector (covering both bores on the east magnet side) and the sunrise micromegas with better performing Bulk and Microbulk technology micromegas detectors. The sunrise Bulk MM detector was installed in December 2007. On the sunset side, one Bulk and one Microbulk MM were installed in February 2008. The necessary infrastructure was built for the three MM detectors: X-ray optics line for the sunrise side, gas systems, electronics and DAQ, shielding etc. All three detectors are taking data for the ^3He run Phase II. The Bulk detectors present excellent background counting rates. The Microbulk has an acceptable background but its active area is limited to half of the magnet bore surface, due to many dead strips from the manufacturing process and possibly edge field effects. The Microbulk will be replaced by a Bulk detector at an appropriate time. Concerning the problematic reflective coatings of the plastic shells for the LLNL 2nd X-ray optics for the MM line, after a campaign of R&D there has recently been some very encouraging developments. A coated shell made by the TS-MME group at CERN has given promising results in the surface analysis tests made at LLNL and a second coated shell is now under test in the X-ray facility at PANTER.

4) Visible measurements at CAST. New groups that joined CAST have undertaken the responsibility for solar tracking at low energies (a few eV). A system based on one Photomultiplier and one Hybrid Photo Diode was installed for two periods of one week each and performed solar tracking and

background measurements. This is the first time that a helioscope operates at these low energies.

5) Analysis and results. The final results from Phase I were published and the ^4He run Phase II analyses are finalized.

6) CAST experimental operation. All the systems necessary for the proper, safe and continuous operation of the experiment were maintained to a good level or even they were improved. The cryogenics system didn't present any problems. The Slow control performed also very well. The GRID measurements confirmed the good magnet positioning with a small offset that can be corrected at the encoder level. A new "solar filming" method, complementary to the previous one, confirmed the solar tracking alignment to within the required precision of one arcmin. All magnet safety requirements set by the previous SPSC report were fulfilled.

A detailed description follows of all the work invested by the collaboration to the advancement of the CAST experiment to this new axion mass domain up to about 1.2 eV.

3. RESULTS FROM THE ^4He PHASE II

3.1 pn-CCD and X-ray mirror system operation

3.1.1 X-ray telescope results ^4He Operation

The analysis of the ^4He data acquired during the data taking period of November 2005 until December 2006 has been finalized. The X-ray telescope was operated during the ^4He run Phase II in the same configuration as during Phase I. The data analysis (Phase II) yields ≈ 295 hours of high quality data taken during axion sensitive conditions (magnet aligned with the sun) and ≈ 2760 hours of background data (magnet not aligned with the sun). The resulting intensity images for tracking and background data are shown in Figure 1. Both images show a homogeneous spatial event distribution over the full CCD chip.

In total, 147 out of the 160 ^4He density steps were completed. The 13 missed steps were covered by the TPC and Micromegas detectors. Both, the detector performance and the mean differential photon flux were stable at a level of $8.66 \pm 0.17 \times 10^{-5}$ counts/s/cm²/keV which translates to 8.12 ± 0.07 background counts per solar tracking on the full CCD chip in the energy range 1-7 keV (see figure 2, left panel). The X-ray telescope can produce an ‘axion image’ of the sun by focusing the X-rays from the magnet bore area (14.5 cm²) to a potential signal area on the CCD chip of $A = 9.4$ mm², improving the signal to background ratio significantly. The expected background in the potential axion signal area is 0.24 ± 0.01 counts per solar tracking in the energy range 1-7 keV. No signal over background could be observed in Phase II (see Figure 2, right panel). The preliminary result of the data analysis of Phase II for the axion-photon coupling constant is shown in Figure 3, the level of the contour line for the axion - photon coupling constant is similar to the expected value.

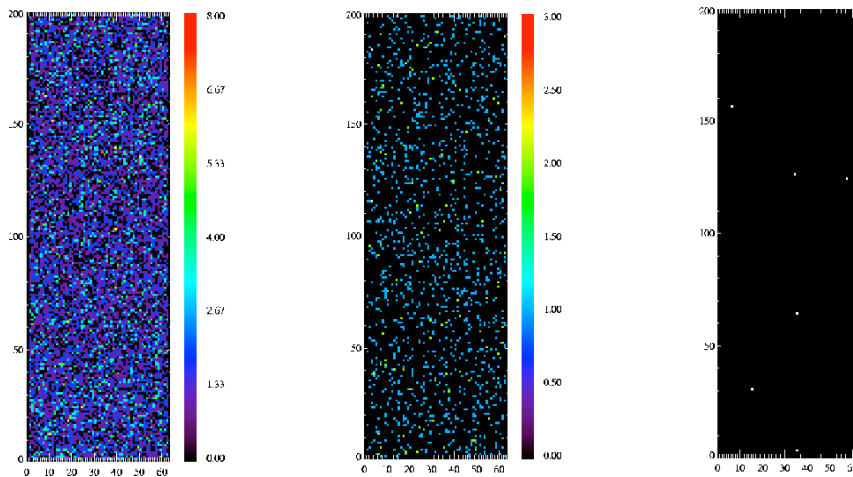


Figure 1: Shown are the intensity images for background (left panel) and tracking data (middle panel) of phase II X-ray telescope data, with exposure times of ≈ 2760 hours for background data and ≈ 295 hours for tracking data. Both images show a homogeneous event distribution over the full CCD chip. The right plot shows the spatial event distribution during a single tracking.

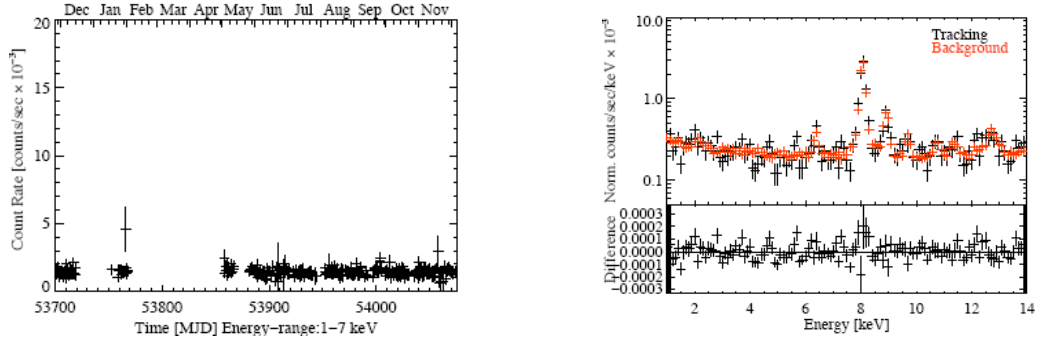


Figure 2: *Left:* Background light curve of the Phase II data of the X-ray telescope. The mean differential flux is stable at a level of $(8.66 \pm 0.06) \times 10^{-5}$ counts/s/cm²/keV in the energy range of 1 to 7 keV, resulting in an expected number of 8.12 ± 0.07 counts per solar tracking on the full CCD chip which corresponds to 0.24 ± 0.01 counts per solar tracking in the potential axion signal area. *Right:* Tracking and background spectra of the X-ray telescope in the energy range of 1 to 14 keV for the same time period. The residuals indicate that both spectra are consistent within statistical errors.

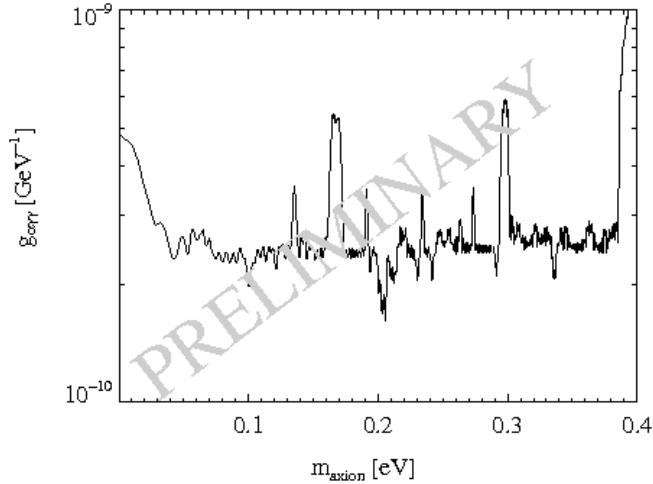


Figure 3: *Preliminary upper limit (95% C.L.) of the axion-photon coupling constant $g_{a\gamma\gamma}$ versus axion restmass m_a , derived from CCD data of Phase II with ^4He in the magnet bores. The peaks result from the pressure setting for which the telescope was not taking data; for these cases a limit can be derived by taking the contribution of neighbouring mass bins into account.*

3.1.2 Verification of the Telescope Alignment 2005-2007

Regular alignment verification measurements were made with an X-ray source (X-ray finger) before, during, and after the ^4He data taking period, to verify the stability of the X-ray telescope's alignment and consequently the stability of the location of the signal spot on the CCD chip. With these measurements we have verified the stability of the axion spot position on the CCD chip with high accuracy (< 1 pixel = 20 arcsec). The results indicate that the aspired stability of the system could be maintained over the whole data taking period.

In autumn 2007 it was planned to install the new Micromegas detector line, including additional shielding components. Since any additional load on the MFB and X-ray telescope platform can lead to a misalignment of the

X-ray optics (platform twists and rotates), we investigated the influence of an additional load on the alignment of the X-ray telescope. Extensive inclinometer and telescope survey measurements (using dummy loads) were done before during and after the Micromegas line installation. The results indicate that a misalignment of 0.097 mrad (maximum tolerable misalignment) corresponds to 150-200 kg additional load on the Micromegas side of the platform, consequently the new Micromegas installation (or a change of the load up to 150-200 kg close to the Micromegas line) will not disturb the alignment of the X-ray telescope.

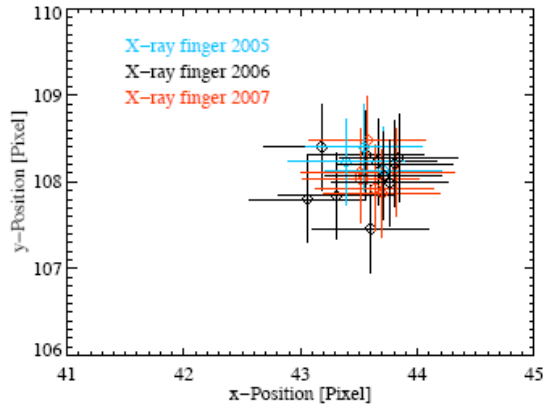


Figure 4: Result from X-ray finger measurements performed in 2005, 2006 and 2007. Shown is the centre of the X-ray spot on the CCD. All measurements done in 2005, 2006 and 2007 yield a precision of the spot position of 1 Pixel (= 20 arcsec).

3.2 ^4He sunrise Micromegas analysis

The sunrise Micromegas detector run continuously during the ^4He run Phase II data taking, covering 159 out of the 160 pressure settings. The analysis of the ^4He run data with the Micromegas sunrise detector has been finalised. The efficiency taking into account all the different contributions (gas conversion efficiency, strongback window efficiency loss, energy resolution and software efficiency) is shown in Figure 5. The integrated efficiency in the 2-7 keV energy range is 44%. The tracking and background energy spectra, after the analysis selection are shown in Figure 6. The difference between the background and the tracking spectra is statistically compatible with no axion signal. The time evolution and the pressure dependence of the background and tracking rates have been studied and prove a remarkable stability within the errors as can be seen from Figure 7. The dependence of the background and tracking rates on the pressure settings in the cold bores for two separate samples, the low energy (2-5 keV) and the high energy one (5-9 keV) is also shown. The bottom plot shows the integrated time spent on each point. Figure 8 shows the background evolution as a function of the day time and the integrated background data samples on each point. Background near the solar tracking is not considered due to the motors induced noise by the fast magnet movement.

Different background definitions have been considered to study the systematic effects and they will be included in the final calculation of the limit. The final limit from the Micromegas analysis is shown in Figure 8.

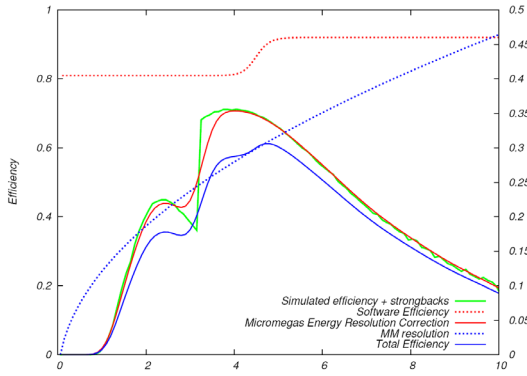


Figure 5: Efficiency as a function of the energy.

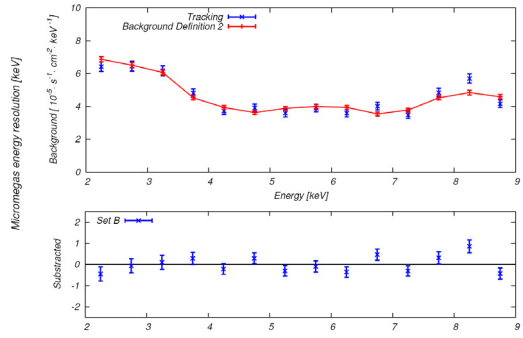


Figure 6: Background and tracking Energy spectra. The difference of the two is shown on the bottom plot.

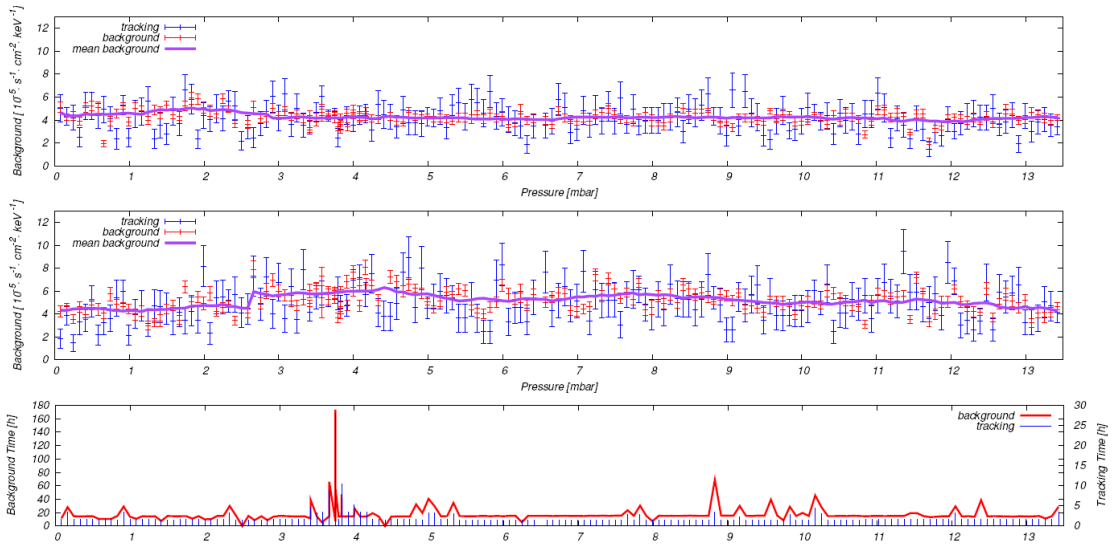


Figure 7: Background and tracking rates evolution as a function of the cold bore pressure. Top plot: the evolution for energies 5-9 keV. Middle plot: the evolution for energies 2-5keV. The bottom plot shows the integrated time spent at each setting.

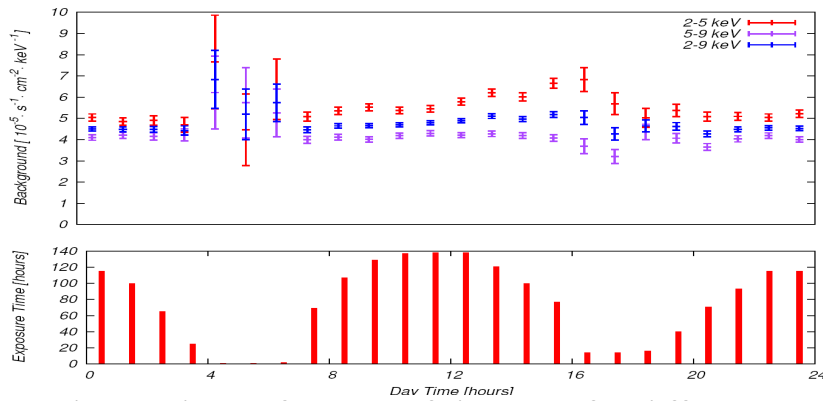


Figure 8: Background as a function of day time for different energy ranges. The lower plot shows the integrated time spent at each point.

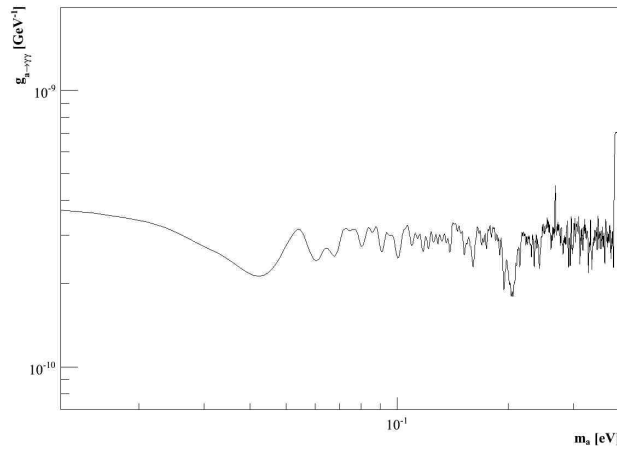


Figure 9: The Micromegas analysis limit on the axion-photon coupling constant (at 95% CL) with ^4He data.

3.3 The ^4He TPC detector analysis

The Time Projection Chamber (TPC) of the CAST experiment operated continuously during the data taking of the ^4He run Phase II. The TPC detector covered 154 out of the 160 pressure settings and recorded tracking data for 304 hours and background data for 4346 hours, representing a 95.75% data taking efficiency. The analysis of the ^4He run Phase II full data sample of the CAST experiment is finalized.

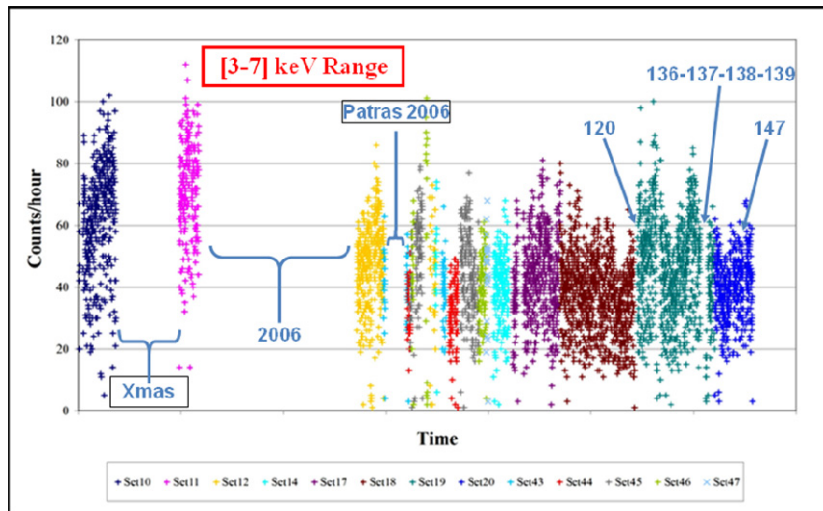


Figure 10: Rate evolution in the 3 to 7 keV range of the TPC detector . The numbers in blue represent the pressure settings lost by the detector due to technical problems. Also in blue can be seen the periods in which the detector had to be dismantled for magnet maintenance.

The stability of the detector rate, in counts per hour, is shown in Figure 10. The TPC data, depending on the different conditions (e.g. seasonal variation of the background induced by the wall) has been analyzed in separate sets that have been combined at the end. Figure 11 shows the evolution of the gain measured in the daily calibration runs. The TPC detector presented a good stability during the whole period of data taking.

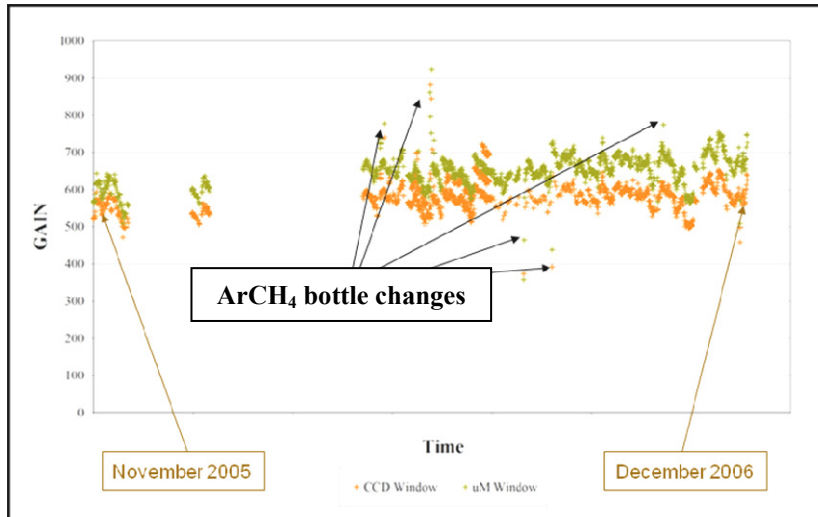


Figure 11: Evolution of the position of the peak of the 5.9 keV peak (^{55}Fe source) in ADC units during the operation of the TPC detector in CAST Phase II.

During Phase II of the CAST experiment, the installation of the cold windows confining the ^4He gas in the magnet bores affected the efficiency of the detector, and therefore, its implications to the analysis had to be considered (see Figure 12).

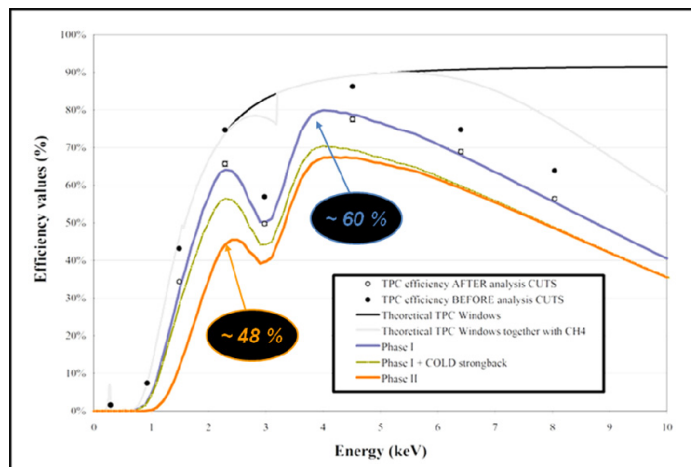


Figure 12: Efficiency of the TPC detector during Phase I and Phase II of CAST. The overall efficiency of the detector considering the expected axion energy spectrum was 60% for Phase I and 48% for Phase II.

The analysis of the TPC data, statistically shows no excess of tracking events above the background level, and therefore only a limit for the axion to photon coupling constant can be derived. A maximum likelihood method is used to produce this limit. The background spectrum together with the ones of the expected X-ray spectra, calculated for different $g_{\text{a}\gamma\gamma}$ coupling strength hypothesis, are compared to the tracking spectrum after being properly normalized. The likelihood method applied to the TPC data covers the range from 1 to 12 keV with a binning of 0.5 keV. The χ^2 (24 d.o.f.) distribution for

the difference between background and tracking spectra is compatible with a null result and follows the theoretical χ^2 of 24 degrees of freedom as expected.

Concluding, the TPC analysis is finalized, and has included the full data sample. The data taking efficiency was 95.75% with an average detector efficiency of 48% and a dead time of 2%. The analysis includes pressure settings up to 13.4 mbar corresponding to an axion mass of 0.39 eV. The final exclusion plot from the TPC detector analysis is shown in Figure 13.

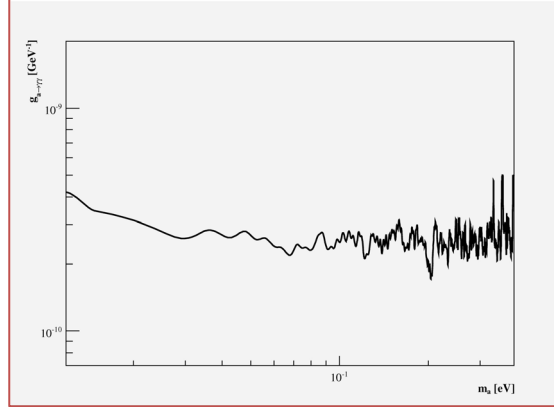


Figure 13: Exclusion plot derived from the TPC data for the coupling constant $g_{a\gamma\gamma}$.

3.4 Combined results

Figure 14 shows the exclusion plot of the combined analyses from the CCD, the Micromegas and the TPC detector. The (red) curve marked ^3He , is the estimated exclusion for ^3He run Phase II. Even though it is not appropriate the indicative “average limit” derived from Phase II is $g_{a\gamma\gamma} < 2.2 \times 10^{-10} \text{ GeV}^{-1}$ which is a “first” for CAST.

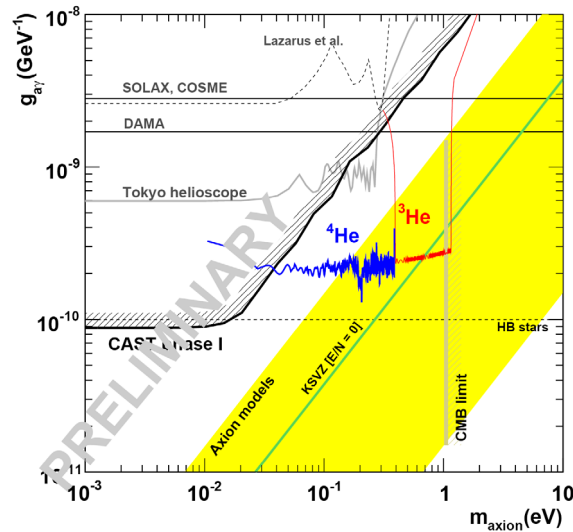


Figure 14: Combined exclusion plot from the analysis of CCD, Micromegas and TPC data, with ^4He as refractive gas in the magnetic pipes during CAST Phase II. The (red) curve marked ^3He , is the estimated exclusion for ^3He run Phase II (2008 – 2010).

4 DETECTORS STATUS

4.1 The CCD Detector Replacement

At the end of the ^4He data taking in 2006 the X-ray telescope was shut-down and stored under save conditions, i.e. flushed with dry N_2 . During the commissioning phase and restart of the system mid 2007, it turned out that the noise of the CCD detector had a critically high level. The noise originates mainly from columns and individual pixels of the CCD with a persistently high dark current and noise (see left part of Figure 15). Extensive performance and diagnostic test performed, indicated that the CCD chip was damaged and had to be replaced. At this time the reason for the defect was not clear. It was decided by the CAST steering committee to replace the CCD chip by a spare part available at the semiconductor laboratory in Munich.

The detector was removed from the CAST magnet and the detector and vacuum system components were investigated in detail for chemical surface contamination (e.g. hydrocarbons) and surface defects. Neither, inside the vacuum housing of the mirror shells and the CCD detector, nor in the pipes and turbo-pumps connected to both vacuum vessels any kind of chemical surface contamination could be found which would explain the damage of the CCD. The visible inspection of the surface of the CCD chip and the shielding components inside the CCD vessel later at MPE revealed surface contamination by metallic micro-particles of a size of typically $100\ \mu\text{m}$. The origin of these metallic particles is an Al-filter installed in front of the ^{55}Fe source which is used to check the energy calibration of the CCD (see right part of Figure 15). This source can be moved in and out of the field of view of the CCD detector with an electro-pneumatic manipulator. We assume that during the 4 years long operation the fixation of the source to the manipulator became loose (mechanical vibrations) and the Al filter scratched on the surface of the vacuum housing of the manipulator while it was moved. At present we consider the resulting Al abrasion as the reason for the defect of the CCD chip.

After the detector has been brought to MPE in Garching, it was disassembled in a clean room and all components were visually inspected. Standardized wipe tests proved that the surfaces of the vacuum vessel and internal shielding were free of chemical contamination. The detector components were cleaned, following a standard procedure for low background applications; finally the material surfaces were inspected and the individual components were out-gassed before we started to re-integrate the detector.

In parallel, a spare CCD chip was tested for basic functionality at the Institute for Astronomy and Astrophysics in Tübingen (Germany) which operates the worldwide only remaining test environment for XMM-Newton type X-ray pn-CCDs. A detailed performance optimization of the chip is not possible with this setup consequently, the final performance optimization of the detector had to be done at CERN before calibrating the detector.

In addition, we decided to re-calibrate the effective area of the X-ray mirror system at the MPE PANTER test facility in Munich in parallel to the detector activities, in order to rule out any degradation of the performance of the mirror reflectivity due to surface contamination. We consider this a crucial step facing a three years long data taking period with CAST. The mirror module was transported to and disassembled at ZEISS before it could be transported to the PANTER facility in Munich. Finally, we could benefit from a unique time slot available in January at the PANTER facility for our

measurements. The results of the calibration measurements indicate that the effective area of the X-ray telescope is still the same as it was measured in 2002, taking an uncertainty of about 10 % into account (the final analysis which requires ray-tracing simulations is still in progress). The final integration of the mirror system was done at ZEISS before the whole system was brought back to CERN beginning of February.

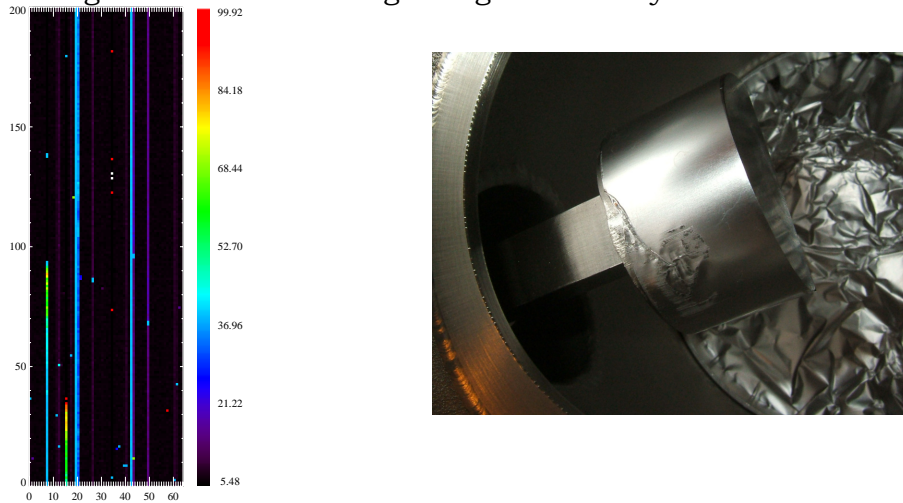


Figure 15: *Left: Noise distribution of the CCD detector after restarting the system mid of 2007. Several columns and pixels show an abnormal high noise level. Right: Manipulator of the ^{55}Fe calibration source. The damaged Al filter is clearly visible.*

4.2 The new pn-CCD detector and the X-ray telescope

4.2.1 Energy calibration of the new pn-CCD detector February 2008

In order to calibrate the new CCD detector, we installed a tuneable X-ray tube in the CAST experimental area, providing different fluorescent emission line energies up to 20 keV. The X-ray tube has been tested and commissioned end of January this year. Beginning of February 2008 the new pn-CCD detector has been calibrated with this source. Several line energies (e.g. Cu-K, Au-M, and Si-K) were measured to verify the gain linearity of the detector. As an example a Cu-K line spectrum is shown in Figure 16 (left panel). The analysis of the calibration data is still ongoing and the final results are expected soon. First preliminary results confirm a linear gain of the detector and an excellent energy resolution of 175 eV at 6 keV.

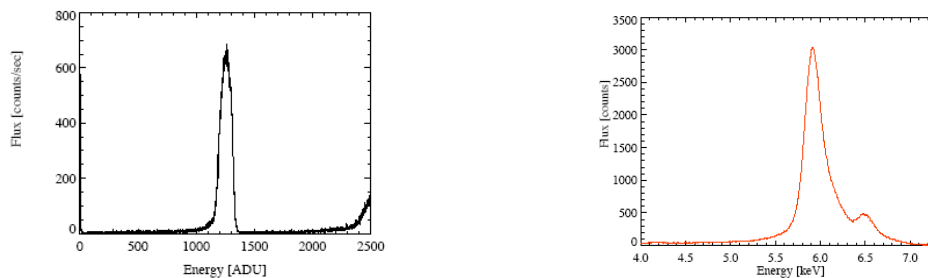


Figure 16: *Left: Spectrum of the Cu-K line acquired with the new pn-CCD detector. For the calibration an X-ray tube was used, providing X-rays with a maximum energy of 20 keV. Right: Mn-K α and Mn-K β line of a ^{55}Fe source measured with the new CCD.*

4.2.2 Alignment of the X-ray Telescope 2008

Mid of February 2008, the X-ray telescope has been installed to the CAST magnet and has been aligned to the optical axis of the CAST magnet. The alignment has successfully been finished at the end of February. The alignment has been verified following a standardized procedure with laser (providing a parallel light beam), geometer survey, and X-ray measurements, using an X-ray source permanently installed on the MRB side of the magnet. Since the count rate of this X-ray source in use since 2003, decreased over time, the old source has been replaced. Figure 17 (left panel) shows the intensity image of this X-ray source, as it has been measured by the CCD. The location of the apparent X-ray spot provides a reference to verify the alignment of the X-ray telescope during the forthcoming ^3He data taking period. The right picture of Figure 17 shows the combined intensity image of the laser measurements and X-ray measurement. Using the projected X- and Y-distributions of these images, the position of the potential axion signal spot is determined.

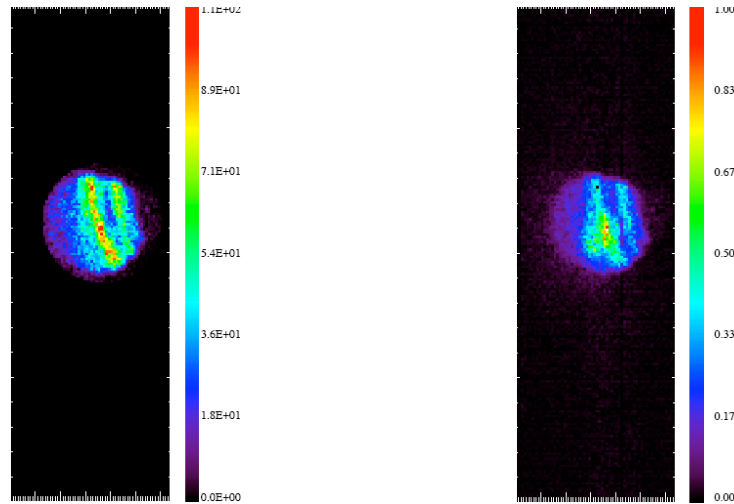


Figure 17: Intensity images from optical alignment of the X-ray telescope done in February 2008. Left: X-ray spot on the CCD chip. A new X-ray source providing a higher count rate was installed and used for this measurement. Right: The combined intensity image of the 2008 X-ray spot and the on-axis laser spot. The position of the centre of the circular axion-signal area is at $X=32.5$ and $Y=11$ pixel with a radius of the circle $r=11$ pixel. The laser spot is slightly offset to the left relative to the centre of the region that encircles the X-ray distribution.

4.2.3 Performance of the New CCD Detector

Based on background and tracking data acquired in 2008, we can conclude that the performance of the new CCD detector is comparable to the performance of the previous CCD detector. The background light curve acquired with the X-ray telescope shows a stable count rate, corresponding to a mean differential flux of $(8.76 \pm 0.16) \times 10^{-5}$ cts/s/cm²/keV (see Figure 18, left panel). In total 414 hours of background data were taken during this year and 2 solar observations could be completed. The energy spectrum shows a homogeneous distribution in the energy range of 1 to 7 keV consistent with the background spectrum of the previous detector (see Figure 18, right panel). The detector performance parameters shown in Figure 19 demonstrate the excellent long term stability of the detector up to now.

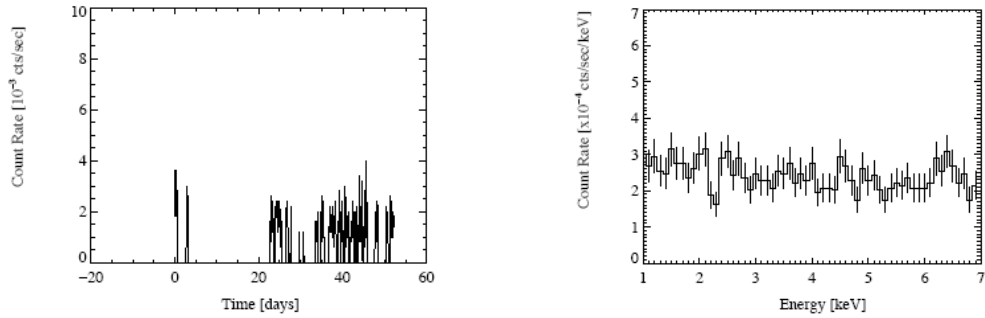


Figure 18: Left: Background light curve observed with the X-ray telescope during operation in 2008. The count rate is stable at a level of 1.45×10^{-3} counts/s in the energy range of 1 to 7 keV. Right: Energy spectra in the range of 1 to 7 keV, derived from background data taken with the X-ray telescope from February until April 2008.

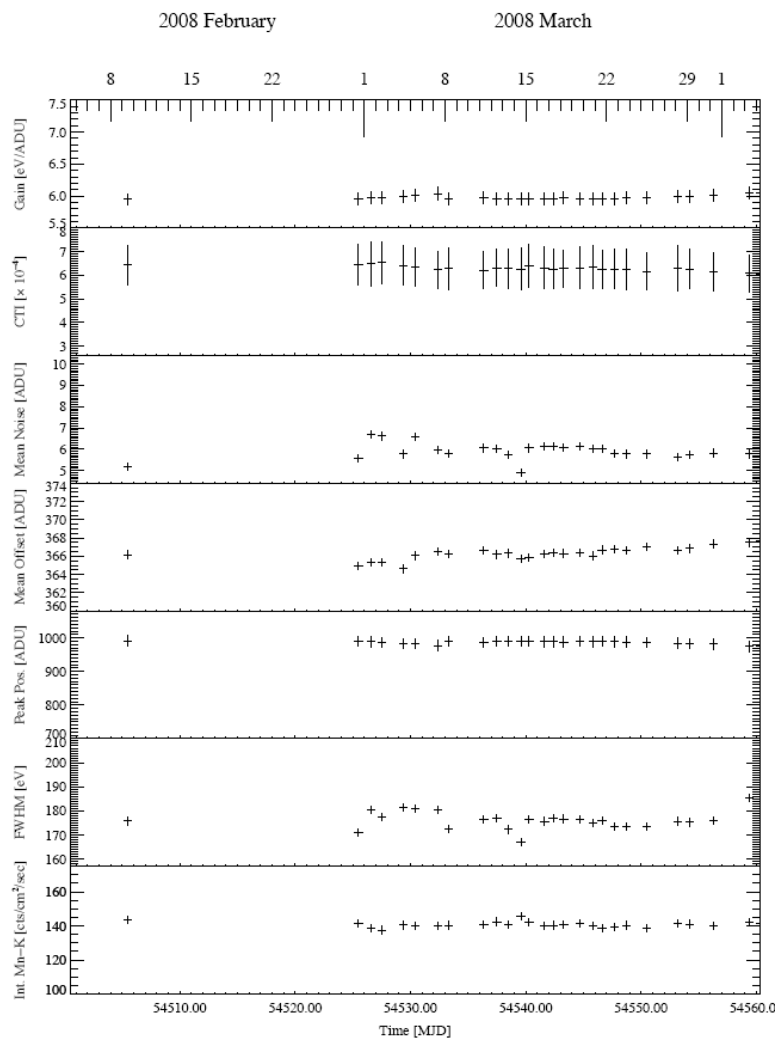


Figure 19: Detector parameters shown from top to bottom: Gain, CTI (charge transfer inefficiency), mean pixel noise, mean offset, the position of the Mn-K α calibration line, the energy resolution and the intensity of the Mn-K α line. The resulting energy resolution is 177 eV at 6 keV and the measured count rate of the Mn-K α line is 140 cts/cm²/s.

4.3 The Bulk and Microbulk Micromegas technology

Since last year the Micromegas group is working on the research and development of a new generation of CAST detectors. Up to 2006 the CAST Micromegas detectors consisted of a copper 5 μm mesh placed on a readout plane at a distance of 50 μm by means of kapton spacers. The manufacturing of this mesh is based on simple chemical-etching techniques on a single foil of kapton copper plated on both sides. The manufacture process relies on the high accuracy of the photolithography technique reached at CERN that allows to print on a 5 μm copper film a grid with 30 μm openings and a pitch of 70 μm ; the kapton is then removed by etching. In a second fabrication, the kapton is partially removed leaving kapton pillars that are used as spacers for the detector amplification gap. In the CAST detectors the mesh was supported by a frame that was held by screws attached to the readout plane. The energy resolution obtained could be quite good (around 20% at FWHM at 5.9 keV) but in practice it was difficult to control the planarity of the whole surface of the mesh. The uniformity of the detector was determined by the way the screws were attached to the readout plane. To achieve better uniformity the CAST Micromegas group decided to invest efforts in recent (Microbulk and Bulk) techniques that could lead intrinsically to a much more uniform detector with lower background.

The Microbulk techniques were very appealing due to the excellent resolution achievable (less than 15% at FWHM at 5.9 keV). Microbulk detectors are built by the same etching technique used for copper meshes as described above, but moreover the readout plane and the mesh are manufactured simultaneously in the same process forming only one entity. As a result, the copper mesh is lying uniformly on the kapton spacers with a very high precision (a few microns) by the manufacturing process. These detectors have shown excellent performance. However they are fragile to sparks and the etching procedure weakens the attachment of the copper strips of the readout plane to the kapton and therefore special care needs to be taken. A few detectors of this type have been manufactured for CAST in the last year. It was the first time that Microbulk detectors were built on a 2-D readout plane which adds complexity to the whole manufacturing process.

In parallel we have also developed Bulk CAST detectors. The Bulk detectors strategy is the same as for the Microbulk detectors: the mesh and the readout plane are one entity. However the Bulk manufacturing process is less delicate as we are dealing with more macroscopic mesh (typically 30 μm thick stainless steel woven mesh) which makes the process more straight forward. The detector is much more robust and the reachable energy resolution is of around 20% at FWHM at 5.9 keV. The energy resolution could be improved if the thickness of the mesh would be reduced.

The two lines of R&D have progressed greatly in the last few months. We believe that for CAST immediate needs (spare detectors) we will concentrate on the Bulk technology.

4.4 The Sunrise Micromegas detector

For the December data taking the new Micromegas line with all subsystems (gas, vacuum, calibration, shielding) were installed and worked at nominal conditions for a few months. However a few days before data

taking a problem appeared during interventions in the line, resulting in a dismounting of the detector and the replacement of the mesh (the active part of the Micromegas detector). The operation was not completely successful resulting in a degraded performance. Nevertheless 9 tracking runs were taken corresponding to 15 different pressure settings. Preliminary results show that in the central part of the detector (~25%) the background rate is comparable to the nominal behaviour of the detector before the intervention. Figure 20 indicates the background level for the December run (100 hours of background and 13 hours of tracking).

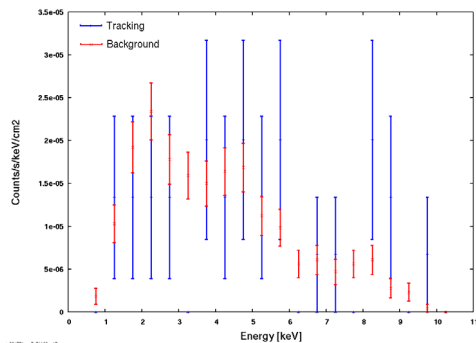


Figure 20: MM Background level for the December 2007 running period

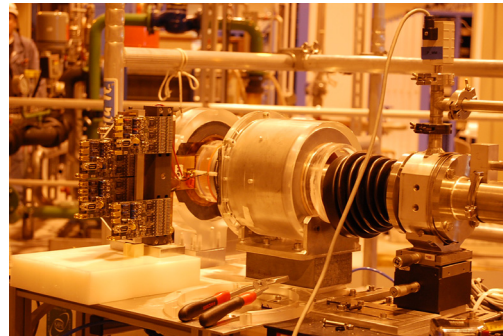


Figure 21. The sunrise MM detector during the February installation

A preliminary analysis of the first 6 runs has been done. The x-y hit map distribution is shown in Figure 22 for background (left) and calibration data (right). In this plot it can be observed that all energy events are uniformly distributed around the space, while in the calibration hit map the vacuum window strong back is visible. Figure 23 shows the background spectra obtained with a preliminary analysis. The level reached is of the order of 2.5×10^{-5} counts/s/cm²/keV and constant during the running period.

In February 2008 the detector used for the December data taking was replaced by a new Bulk type detector to improve its performance and its active area. A photo of the installation is shown in Figure 21. The background level was improved to 1.77×10^{-5} counts/s/cm²/keV.

The detector is now running with a non-flammable mixture (Ar with 2% Isobutane) with an over pressure of 1.4 bar. This over pressure increases the detector efficiency by around 9% in the 2-7 keV range.

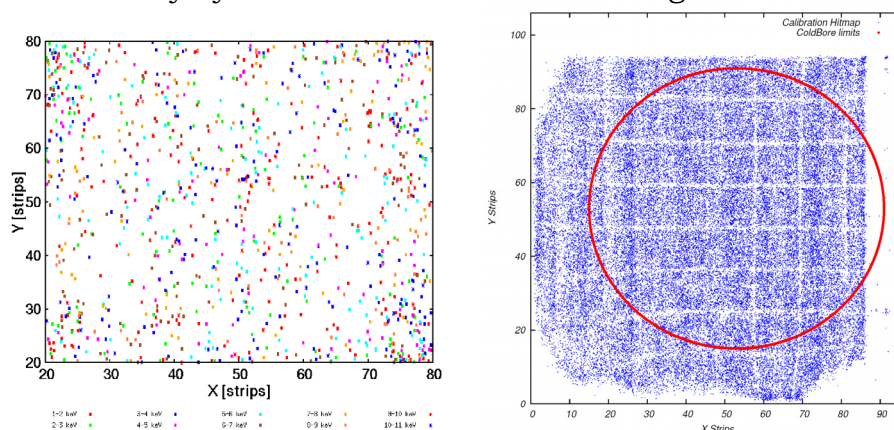


Figure 22: The sunrise MM event distribution in the x-y plane for background (left) and for calibration (right). The (red) circle represents the cold bore area. The vacuum window strongback is “imprinted” on the plot since the detector is irradiated from inside the vacuum.

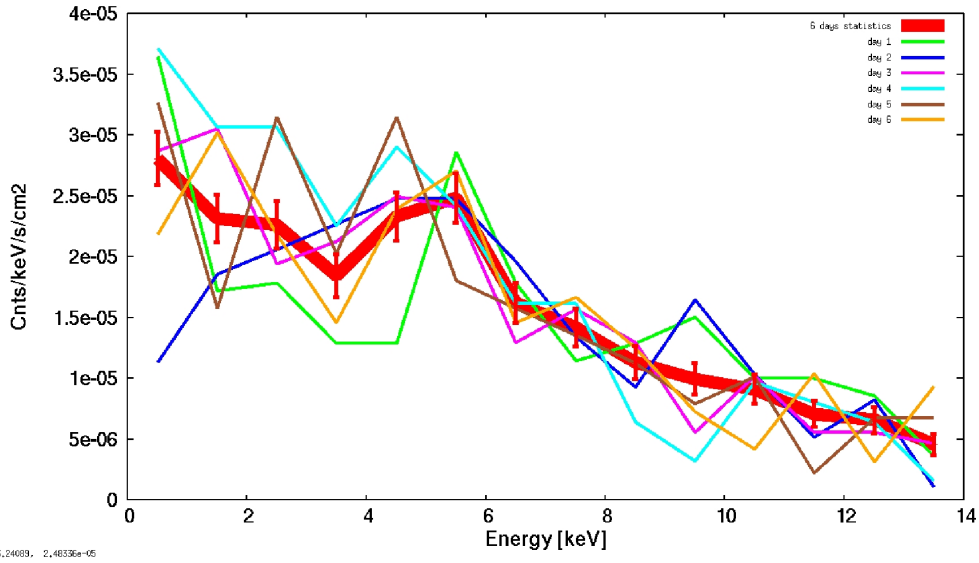


Figure 23: Sunrise MM energy spectra for the first 6 background runs. The (red) thick line shows the level for the cumulative statistics.

4.5 The Sunset Micromegas detectors

The infrastructure for the new Sunset Micromegas detectors was installed in December 2007. All the subsystems gas, vacuum, calibration system, interlocks, data acquisition were working at nominal conditions. The system was not fully operational for the December data taking and the time was used to improve the interlock systems and detectors. A photo during the mounting is shown in Figure 24 (left). During the first months of 2008 the gas and vacuum system were improved minimising leaks. The detector drift windows were changed for thicker windows in order to minimise gas diffusion to the magnet. Finally a Microbulk detector was installed and a Bulk detector. The shielding was the last piece that completed the commissioning as seen in figure 24 (right).

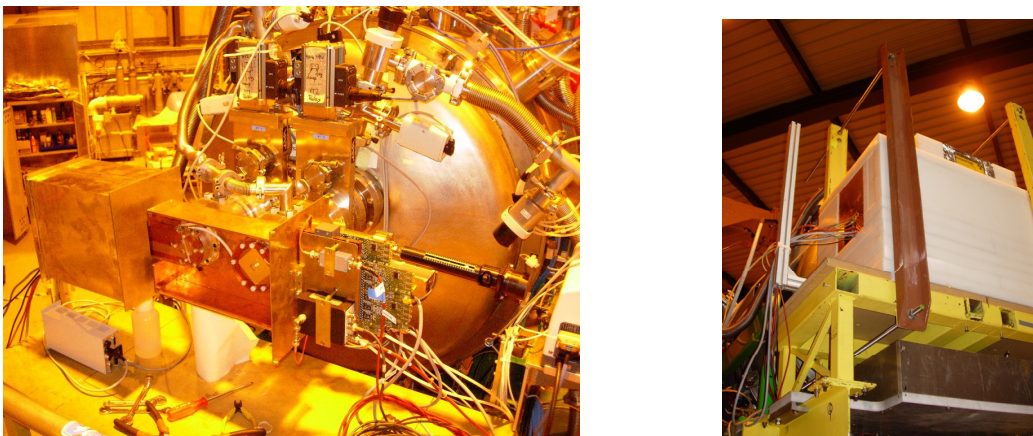


Figure 24, Left: The sunset MM detectors during the installation. The MM detectors on the left are surrounded by a faraday cage while on the right the electronics cards are not covered yet. Right: the final installation of the shielding is shown.

The data acquisition system was built to read out both micromegas detectors simultaneously. It is similar to the sunrise DAQ, with a faster VME controller (CAEN V2718) and an optical link to the control room for communication and data transfer. The dead time is about 1% at the CAST rates. The system performs data taking, online event display, online monitor for both micromegas, automatic calibration and is working in autopilot or manual mode. In autopilot mode (default data taking mode) a scheduled sequence of runs (pedestal, calibration MM1, calibration MM2 or Tracking/cosmics) in any requested order is performed repeatedly on a daily base and the data are transferred to the CASTOR archiving system. The system has been tested to run without intervention for more than two months. Figure 25, on the left shows the DAQ hardware (VME, NIM crates and optical link) and on the right a snapshot of the control and the online event display.

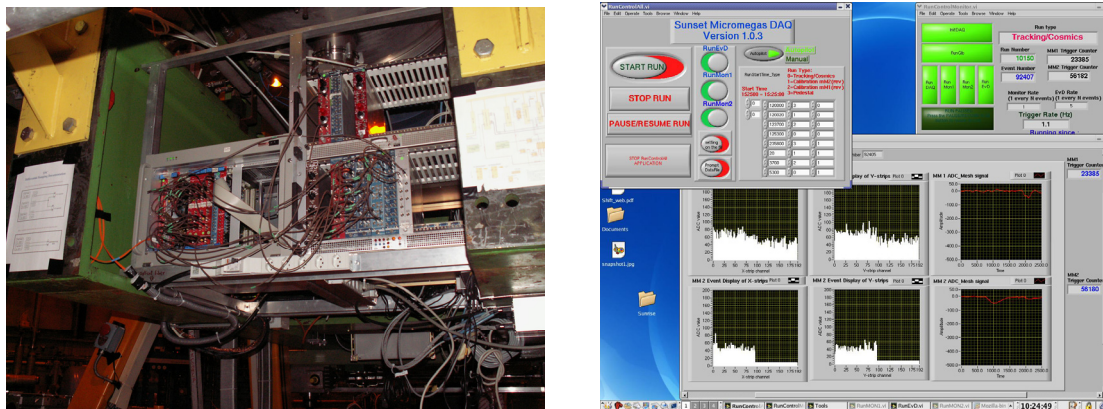


Figure 25. Left: The DAQ hardware (VME crate, NIM crates and optical link) are shown as they are installed under the sunset micromegas magnet side. Right side: a snapshot of the control and the online event display is shown.

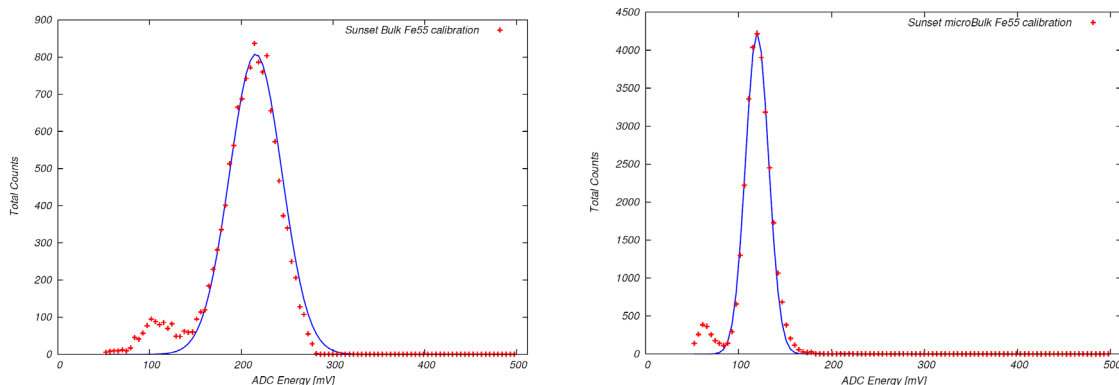


Figure 26. Plots of energy spectra acquired with the ^{55}Fe source for the sunset Bulk MM (left) and the sunset Microbulk detector (right).

The energy spectra for each detector obtained with the calibration ^{55}Fe source is shown in Figure 26, and summarized in Table 1. Even though their resolution is not optimized, we should note that the background rates are very low for the Bulk and satisfactory for the Microbulk MM Figure 27 and Table 1. The micromegas group is building four Bulk MM detectors one of which will replace the sunset Microbulk and the rest will serve as spare and for further laboratory tests. The

Microbulk MMs have presented a background level of the order of a few 10^{-6} but they are difficult to recover when they fail (e.g. after sparking) and present weaknesses on the x-y strips structure. The MM group is working hard to overcome these problems in which case a great improvement of the sensitivity will be offered to the CAST experiment.

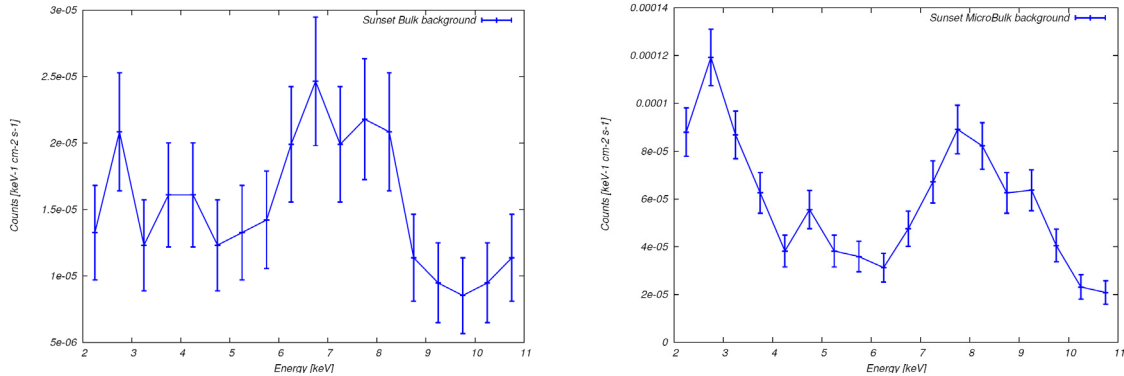


Figure 27: The background level for the sunset Bulk MM (left) and the sunset Microbulk MM (right).

Detector	Background (cts/s/cm ² /keV)	Energy Res. Ampl. (%)	Energy Res. Int. (%)
Bulk MM Sunrise	$(1.77 \pm 0.11) \times 10^{-5}$	26.6	25.9
Bulk MM Sunset	$(1.74 \pm 0.18) \times 10^{-5}$	28.1	27.7
Microbulk MM Sunset	$(6.38 \pm 0.31) \times 10^{-5}$	27.7	28.0

Table 1: The background rates and the energy resolution at 5.9keV for all three MM detectors.

4.6 The MM line X-ray optics status

During the last year, the LLNL team has focused attention on identifying a coating technology that can deposit smooth metal coatings on the integral shell, polycarbonate substrates. To support the evaluation of coating methods, LLNL produced several test articles that are identical to the length and diameter of substrates needed for the CAST optic. These parts were then used to explore two deposition methods: RF sputtering of iridium, performed by researchers at NASA Marshall Space Flight Center and magnetron sputtering of gold, performed by researchers at CERN.

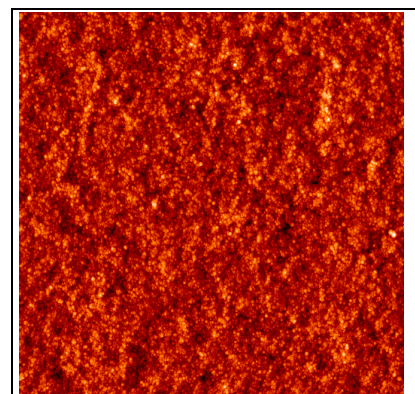
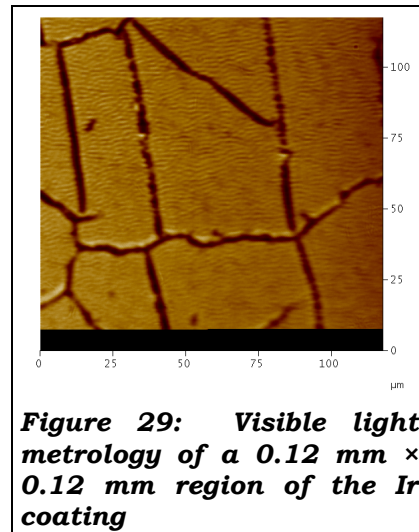
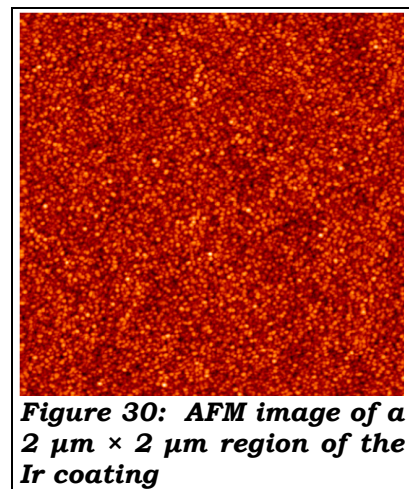


Figure 28: AFM image of a 2 μm × 2 μm region of the Ir coating

The NASA group developed Ir sputtering in support of NASA missions, and more recently has expanded their use to a number of applications, including a collaboration with LLNL for biomedical optics. NASA MSFC generously offered to try their RF sputtering technique on the LLNL substrates. After deposition, the substrates were returned to LLNL where metrology was performed to evaluate the roughness of the coatings. Figure 28 shows a $2\ \mu\text{m} \times 2\ \mu\text{m}$ region of the Ir coating obtained via AFM. The roughness at this position is $9\ \text{\AA}$ rms. At other positions, the roughness was as high as $20\ \text{\AA}$ rms. This level of high-spatial frequency error is right at the limit of what is needed for CAST. Unfortunately, the low-spatial frequency errors are much more problematic. Figure 29 shows a $0.12\ \text{mm} \times 0.12\ \text{mm}$ region examined under visible light. The “cracking” presents a serious impediment for use as an X-ray mirror.



The CERN group, led by Sergio Calatroni, used their vast experience to develop a novel approach for magnetron sputtering thin, uniform gold coatings on the interior of the polycarbonate substrates. Starting with proven approaches for other applications, they systematically tuned their process to work on glass substrates. Glass has similar conductivity properties as polycarbonate, and thus serves as a good surrogate for the LLNL substrates. Once the CERN group had finished their development work, they deposited thin gold coatings on the same size cones needed for CAST, and then sent them to LLNL for metrology. Figure 30 shows a $2\ \mu\text{m} \times 2\ \mu\text{m}$ region of the Au coating obtained via AFM. The high spatial frequency was in the range $10\text{--}13\ \text{\AA}$, which is right at the specification for the CAST optic. Equally important, the “wrinkles” seen in the MSFC coatings were not present in the CERN gold coatings.



Based on the metrology of the test-article coatings, the baseline for future CAST optics will be to use the magnetron sputtering technique, developed at CERN, to deposit thin gold coatings on the polycarbonate substrates. LLNL will continue to seek institutional support to continue working on a second X-ray optic.

5 THE ^3He GAS SYSTEM STATUS

The ^3He gas system is a necessary upgrade in the CAST experiment to extend the axion search up to the rest mass $m_a \approx 1.1$ eV. It presents two major challenges: the accuracy required in measuring the quantity of gas introduced into the cold bores, and the need to operate the system so as to avoid any loss of the expensive gas.

The data taking runs with ^4He provided essential input for the design of the ^3He gas system, described in the Technical Design Report (CERN-SPSC-2006-029). This was successfully reviewed by an expert Review Committee, which provided additional technical and operational suggestions and several safety recommendations that were incorporated in the final design.

Based on the experience gained during the operation with ^4He , and on the quench tests before constructing the ^4He gas system, the main requirements for the design of the ^3He gas system have been set: safety against loss of ^3He , accurate metering of the amount of ^3He in the magnet bores, absence of thermoacoustic oscillations and protection of the thin cold X-ray windows during a quench.

The system philosophy is based on a closed hermetic circuit, running normally at a pressure below 1 bar and divided in 4 sections as shown by Figure 31:

- The cold bore region where the gas is confined and maintained at stable density
- The metering region where the quantity of gas sent to the cold bore is accurately measured
- The expansion region for a fast recovery of the gas in case of quench.
- The storage region where the necessary inventory of ^3He contained.

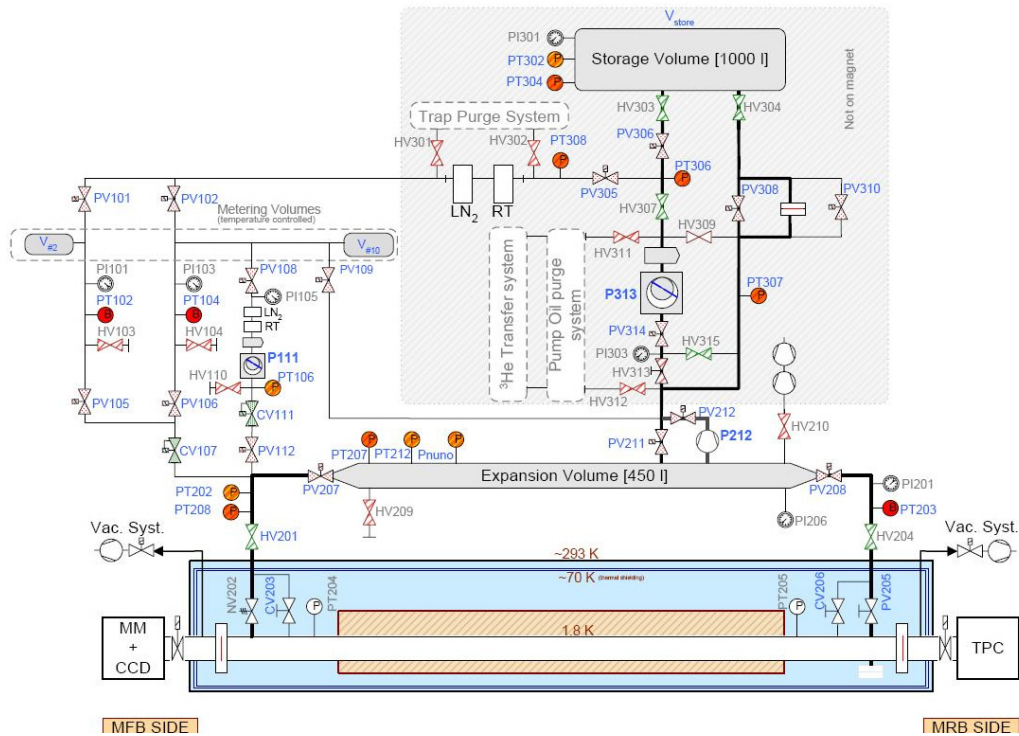


Figure 31: Schematic diagram of the ^3He gas system

In the cold bore region the gas is confined and separated from the vacuum in the beam lines leading to the X-ray detectors by cold thin X-ray windows that should withstand the pressure difference that develops in the worst case of incidents. The development of these elements was done by SACLAY and CERN CAST and cryogenic testing and optimization of these elements was done by the CERN Cryolab and revealed that they are suitable to comply with both mechanical and leak-tightness requirements. One of the windows was successfully pressure cycled up to 3.5 bar, providing additional confidence, since the gas system protection is designed in such a way that the maximum differential pressure should not surpass 1.2 bar (the maximum pressure that can develop in the cold bore after a magnet quench in the case that all safety systems fail is estimated to be 1.25 bar (end 2008) and 2.5 bar (end 2010)).

The metering region not only provides the mechanism for accurately measuring the quantity of gas sent into the magnet cold bores, but also allows flexible modes of operation, ensuring the possibility to make two density steps per day, either by changing the density before or in the middle of the tracking run, or to ramp at constant speed the gas density up or down during the tracking period, covering a maximum of 10 steps during the run.

The number of density settings has been optimized to maximize the discovery potential, by overlapping the axion mass distribution at about one FWHM between two consecutive density settings, and corresponds to a pressure difference of ~ 0.1 mbar at 1.8K. The possibility to make double stepping per day comes from the need to shorten the data taking period to exploit the full available range with ^3He before the end of 2010.

These new operation modes also allow the experiment to be more flexible in case of a potential signal or the need to reject that hypothesis, allowing an easy way to revisit a given density setting or to make smooth scans around a density region.

The integration of the new ^3He gas system required major modifications inside and outside the cryostat.

Inside the cryostat, significant integration studies were done in order to accommodate all the new elements. The necessary modifications included a complete re-routing of the pipes that link the cold bores to the outside of the cryostat, with the introduction on both extremities of new cryogenic elements.

At the MFB end, a cryogenic check valve and a cryogenic needle valve, plus new thermometry and heaters. At the MRB an electro-pneumatic cryogenic valve and a cryogenic needle valve, plus a cryogenic rupture disk and new instrumentation such as a new pressure transducer for measuring thermo-acoustic oscillations and new thermometry and heaters.

This intervention required the removal of the old pipework, by cutting the lines, and installation of the new pre-assembled lines by welding. Some of the welds required state-of-art techniques and skills.

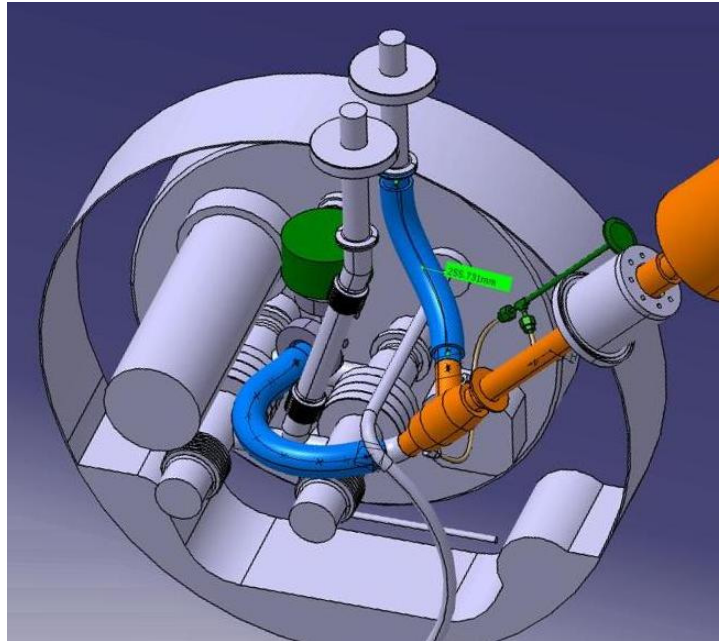


Figure 32: Detail of the modified 3D model inside the Cryostat (MRB side)

One of the limiting items that delayed the closure of the cryostat was the late delivery of the cryogenic rupture disk that ended up by failing the test of inverse pressurization (not required for the normal operation, but needed for a good leak testing). Another company was contacted and, in order to avoid further delays, the new cryogenic rupture disk will be mounted in a future intervention when the cryostat will need to be opened again.

In addition, the magnet Liquid Helium cooling line had to be re-routed to allow the passage of the body a new cryo-valve, which required cutting, welding and pressure testing.

One of the main constraints for this intervention was the very limited space (Figure 33) for the required operations such as cutting and welding, in such a delicate region. All these factors permitted the cryostat to be closed in the month of June 2007.

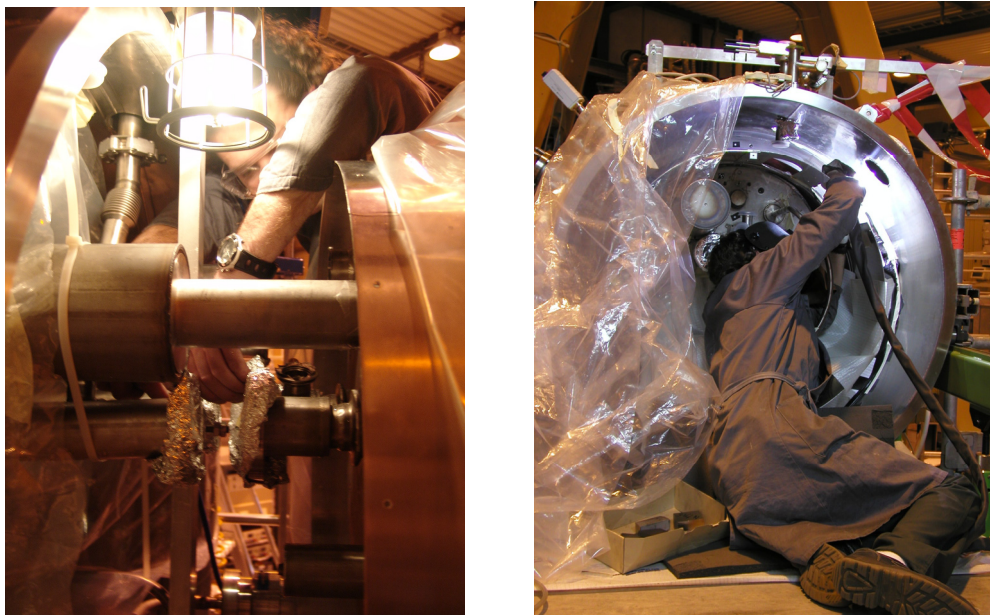


Figure 33: Intervention done in the very limited space inside the CAST cryostat, done by excellent MWS technicians

Outside the cryostat lies most of the gas system components, with metering volumes, storage and expansion vessels, plus vacuum pumps and instrumentation. These components are non-standard and they were designed in such a way as to avoid any interference with the magnet movement, or support structures, while minimizing additional loads on the magnet supports. These components were produced with the help of the CERN main workshop (CMW).

The production of the gas metering region, with its very compact design and high quality requirements, was delayed by the late delivery of miniature hermetic bellows-sealed electro-pneumatic valves, which occurred in late July.

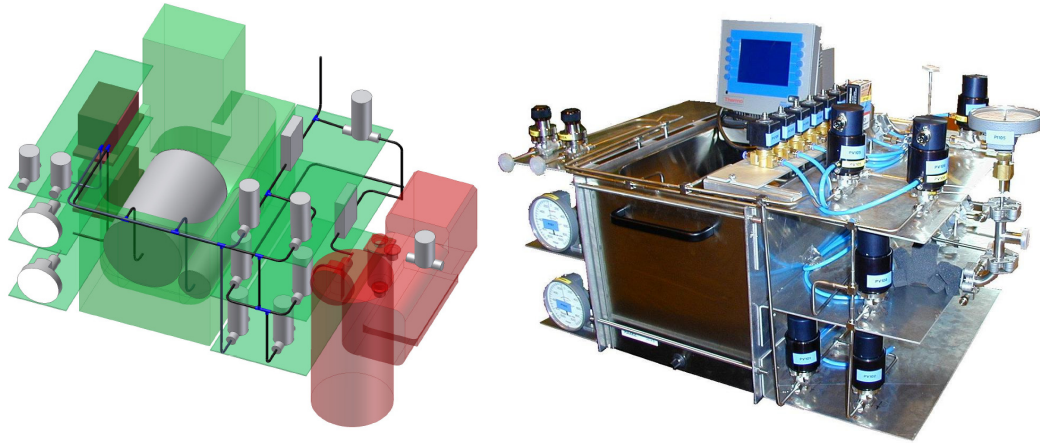


Figure 34a – 3-Dimensional model of the Gas Metering Panel

Figure 34b – Picture of the Gas Metering Panel before placed on its final platform

The assembly, with over one hundred precision orbital weldings was then carried during the summer period where most of the CMW personnel was away or requested for LHC, with great sacrifice in the end of August the equipment was assembled and brought to the area for integration with other pre-assembled pipework.

In parallel the control and supervision system was conceptualized, to include all the safety and routine operating modes, the size of the PLC has been established and the ordering and delivery of equipment.

Once all the hardware was laid on the area, the cabling of instrumentation started with the help of AT-ECR-CO, connecting all components to a unique PLC.



Figure 35: Positioning of the Expansion Volume on top of the cryostat with the help of the crane.

All the necessary ^3He needed for the CAST physics runs has first to be transferred to the Storage Volume which is dimensioned to keep the gas pressure below atmospheric (~ 1000 litres volume), the gas can then be pumped into the metering volumes. During a magnet quench the gas also needs to be recovered from the expansion volume into the storage volume.

This region consist of a hermetic rotary vane pump for ^3He , an oil mist filter, two activated charcoal traps at room temperature and liquid nitrogen temperature, 13 electro-pneumatic valves, pressure and vacuum gauges and an optimized pipework routing (Figure 36).



Figure 36: Picture of the Storage and Recovery region.

Because of the increasing number of equipment using compressed air, the compressed air supply was reorganized, with a dedicated buffer volume for the ^3He gas system and at each end of the magnet, 2 dedicated manifolds that supply each individual electro-pneumatic valve in the gas system.

To bring together the large number of new signals (over 100), the electrical and signal cabling was made by experts (AT/ECR). The new cabling was laid down in specific trays and joined in 3 different interconnection boxes placed on different zones of the experiment. From the interconnection boxes the different signals connect to a new electrical rack which is managed by the ^3He Gas System PLC (Programmable Logic Controller).

To allow a better monitoring of the different states of the gas system inside the cryostat, an upgrade to the instrumentation was done, where new calibrated temperature sensors, pressure transducers and heaters were positioned in interesting regions.

The n-Rack that was used for the ^4He data taking runs received a major upgrade to include the increasing number of signals and as consequence the DAQ had also to be upgraded (Fig.37)

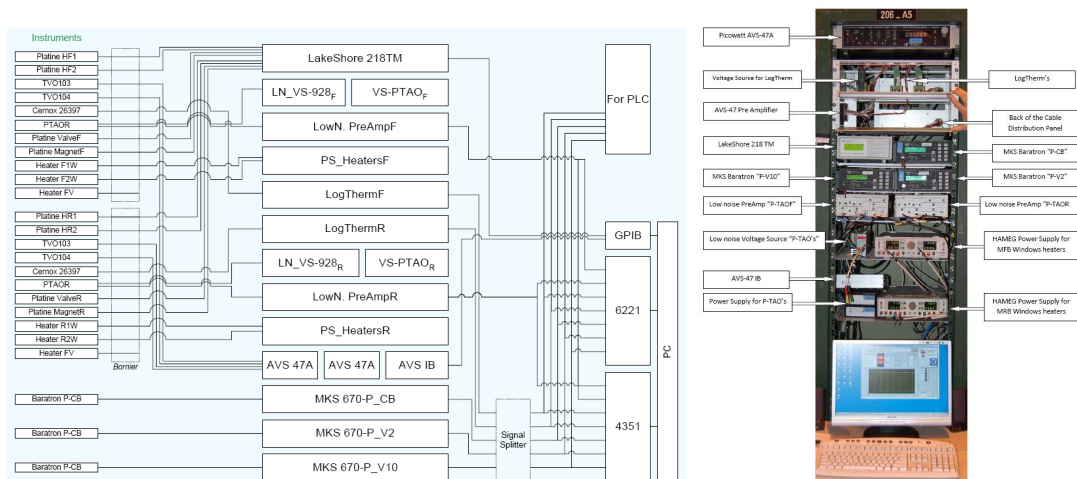


Figure 37: Schematic diagram of the cabling & instrumentation inside n-Rack and photo of the rack

This rack also works as interface between the new Gas System PLC and the existing Slow Control of the experiment.

Due to the complexity of the ^3He gas system, the large number of signals, possible operations and large number of instruments to monitor, it was decided to use a PLC for the Control and Supervision of the gas system.

The PLC allows the remote operation of valves and pumps using a computer interface, it will also allow the initialization of pre-programmed operations that have to be done routinely, as well as the data logging of equipment states, pressures, etc.

The ^3He Control System was designed by AT/ECR/EC using UNICOS, the CERN standard control architecture for cryogenics (UNICOS = UNified Industrial Control System). It provides flexibility and facilities operation due to a standard design interface, and it ensures a smooth long term operation, by the support and expertise given by the resources at CERN.

It is based on simultaneous generation of PLC and SCADA devices, diagnostics tools, and "object-oriented" programming with specific hierarchy, and results rapid prototyping and optimal regeneration mechanisms.

The ^3He Control system also benefits from the LHC_logging, for long term archiving and TIMBER Interface for process data analysis, which also allows with any web application the visualization of the history of equipment status and readings trends.

After the PLC cabling finalized and debugging all the signals, the commissioning phase started, where the whole system was first put under vacuum and carefully leak tested, after that the operation of each individual component was tested. Some problems occurred in the operation of the mass flow controllers, which caused the damage of the electronic cards; these had to be sent to the producer to be repaired.

Next, the system was filled with ^4He and the testing of all operations with the PLC was done. Tests were done to search for spontaneous thermo-acoustic oscillations which show very good results for the coming runs with ^3He .

The behavior of the gas during step fillings and its stability along the magnet cold bores were also tested.

The recovery of the gas was also tested during a magnet quench at 12.8kA. This test showed a very fast reaction of the system on rescuing the gas from the magnet

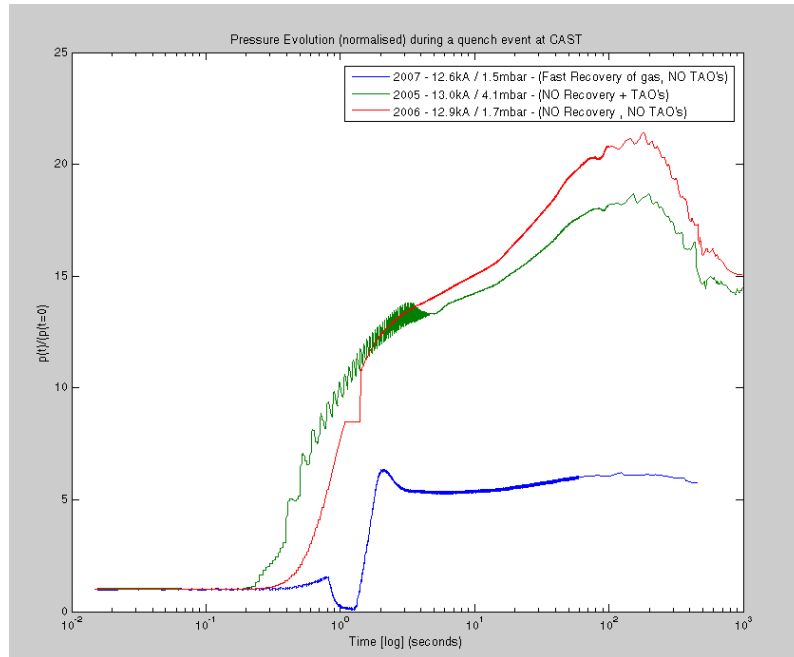


Figure 38: Pressure evolution during a magnet quench with ^4He in the cold bores. The plot shows the normalized pressure increase $p(t)/p(t=t_0)$ as a function of time, being $t=t_0$ the quench time.

cold bores into the expansion volume, the pressure increase factor is only ~ 7 , when compared the increase factor of ~ 20 without recovery.

A data taking period took place in December with ^4He in the cold bores, covering some of the missed settings by some detectors and where shifters gave very good feed back about the operating procedures, which helped to make the user interface simpler.

With the start of 2008, one third of the full amount of the ^3He gas provided by LLNL was transferred from the transport cylinder into the system. After the magnet was put back into nominal operating temperature, a series of tests and operations followed, which was finalized by sending 50 mbar at 1.8 K into the cold bores.

Since Nuno Elias, will soon start a new job outside CAST, training has been being given to CAST collaborators and AT-CRG collaborators, so that the knowledge which was gathered is kept among those using the system.

Data taking with ^3He gas in the magnet cold bores started in the end of March after the installation of 3 new Micromegas detectors and revamping of the CCD detector. One natural quench of the magnet triggered the safe evacuation of the ^3He gas into the expansion volume.

At this time, contamination of air in one of the volumes was detected, which required a fast repair and in order to assure purity better than 1 ppm, 39 cycles of gas purification were repeated. The success of these shows the design is good and flexible, and the operation allows diagnosing and solving undesired scenarios. After the quench and repair the ^3He was re-metered and CAST is back into data taking.

The ^3He gas system is fully operational and will be used in the data taking runs up to the end of 2010 with very small improvements.

6 THE VISIBLE MEASUREMENTS AT CAST

In order to extend CAST performance to detect visible (~ 3 eV) photons generated in the CAST magnet by possible interactions of low-energy solar axions, we have optically coupled to the CAST magnet bore a prototype detector system sensitive to \sim eV photons. The measurements aimed at studying the background level and perform solar tracking and were performed in November 2007 and in February / March 2008

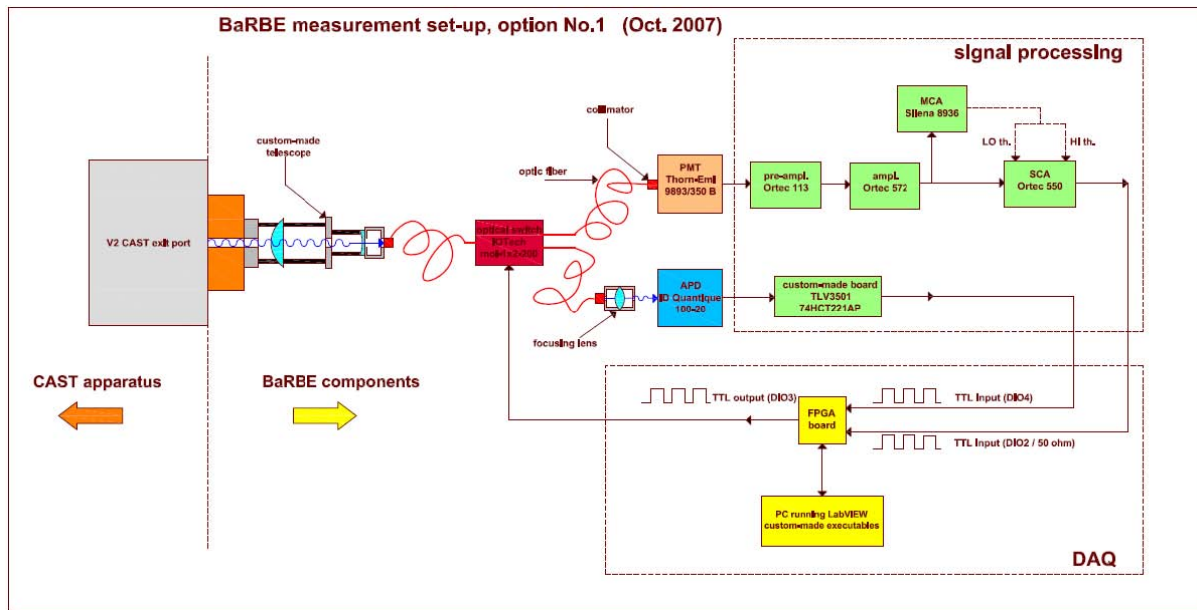


Figure 39: Schematic layout of the BaRBE measurement setup. The Galileian telescope, the optical switch and the two detectors are shown.

BaRBE Experimental apparatus

The basic idea is to share the same magnet exit port between two different detectors, initially a photomultiplier tube (PMT) and an avalanche photodiode (APD). The light collected from the CAST magnet bore with a telescope is coupled to an optical fiber connected to an optical switch. By applying a TTL signal to the switch, output 1 or 2 can be chosen: in this way each detector acquires data half the total tracking time, while in the other half it acquires background data. The setup is optimized to work in the visible range and its layout is schematically shown in Figure 39

The main components of the setup are:

- Galileian telescope, consisting of a 2 inch dia. $f = 200$ mm and a 1 inch dia. $f = -30$ mm lens, used to couple light coming out from the CAST magnet bore into an optical fiber. The coupling efficiency is in the range 40% to 70%.
- optical switch (LEONI mod. 1x2, 50 Hz maximum switching frequency, 10 ms switching time, 1 IN and 2 x OUT pigtailed fibers equal to main 40 m fiber – multimode 200 micron core, 200 – 1600 nm transmission range, 0.9 dB insertion loss); the switching is controlled by a TTL signal (given by a PC desktop through an FPGA board).

- Thorn-EMI 9893/350B PMT (peak sensitivity at 350 nm) with a measured dark count rate (DCR) of 0.4 Hz when operating at 1950 V of bias and at $T = 273$ K.
- id-Quantique model id100-20 APD detector (0.4 Hz measured DCR, 20 micron active area diameter, 500 nm peak sensitivity); the default -2 V, 10 ns output signal is converted to a standard TTL signal by a custom circuit; presently the focusing optics is not optimised and the efficiency is therefore reduced by a factor up to 100.

Data are acquired via a National Instrument 7831R FPGA board with in-house developed Labview 8.2 software controlling both switching frequency and acquisition time, and giving the total counts for the two detectors separately.

Detector alignment and preparation

Before each run the telescope was aligned to the CAST magnet axis: a reference axis, having a known position with respect to the optical axis, is marked on the telescope assembly. The reference axis is then aligned, with the help of the surveyors, in such a way as to have the optical axis parallel with the magnet axis. The final misalignment between the magnet axis and the optical axis of the telescope is 1.2 mm in the horizontal direction and 1.6 mm in the vertical direction. Given the 0.3 rad telescope input acceptance angle this is considered as satisfactory. After final positioning, the PMT, the APD and the optical switch were shielded with thick black cover. The optical fiber was covered with a plastic sheath and then placed inside metal tubing. Finally, a LED source was placed inside the telescope cover in order to check the integrity of the light transmission chain.

Measurements

For each of the two runs the data sets can be divided in:

- Background data (indicated in plots as BGR), typically 30000 s long and conducted during night time.
- Dummy Solar Tracking (DST) data; in these measurements the magnet aperture followed the same curve as in actual solar tracking but without pointing at the sun.
- Solar Tracking (ST) data (each data taking was roughly 5000 s long).

Data analysis and results

Since the APD data are of inferior quality due to poor focusing, only the PMT measurements were considered. The total number of counts in each measurement is affected by afterpulses generated either by the PMT itself or by its readout electronic chain. It was estimated that afterpulses account for about 11% of total counts.

To eliminate the effect of the afterpulses the mean rate of counts was calculated, for both “light” and “dark” counting regimes by solving for $x = 0$ the equation $N_x = A \cdot e^{-m} m^x / x!$, where x is the channel number, A is the total number of occurrences in all channels, N_x is the number of occurrences in the x -th channel measured experimentally. In this way, occurrences in channel 0 are not affected by afterpulses.

Summary of November 2007 run

- detector chain attached to the CAST VT1 gate valve port
- preliminary tests to check the light transmission chain. Lights in the experimental hall were found not to influence the measurements
- background measurements in different magnet positions and with the field on and off
- about 10000 s of Dummy Solar Tracking data
- about 35000 s of actual Solar Tracking data
- results summarized in Figures 40 and 41 below

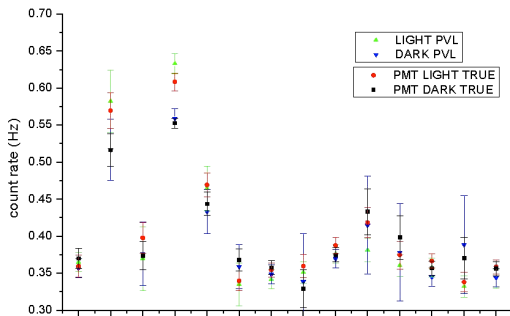


Figure 40: Count rates in the November 2007 run.

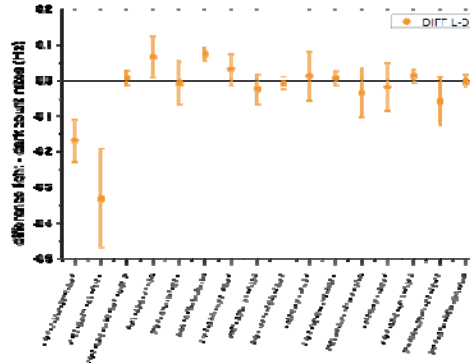


Figure 41: Difference between background and solar tracking data.

Figure 36 shows the count rates in the November 2007 run. LIGHT and DARK labels indicate data taken with the detector either looking at the magnet bore or being blocked by the switch, respectively. TRUE labels rates calculated using the method indicated in the text, while PVL labels rates not corrected for afterpulses. The first 5 data sets should not be considered, as they represent preliminary tests. The horizontal axis represents time. Data points referring to background or solar tracking data are plotted together, indicating the fact that no excess of counts is seen when tracking the sun.

In Figure 41 each point represents the difference between tracking and background count rates for the full data set. The first two sets at left were acquired with a preliminary setup and should be disregarded.

Summary of February/March 2008 run

- detector chain attached to the CAST VT2 gate valve port
- background measurements in the two magnet parking positions and with the field on and off
- about 5000 s of Dummy Solar Tracking data
- about 40000 s of actual Solar Tracking data; 20000 s were taken with the magnet pointing off-center of the sun, half 0.25° to the right and half 0.25° to the left.
- results summarized in Figures 42 and 43 below

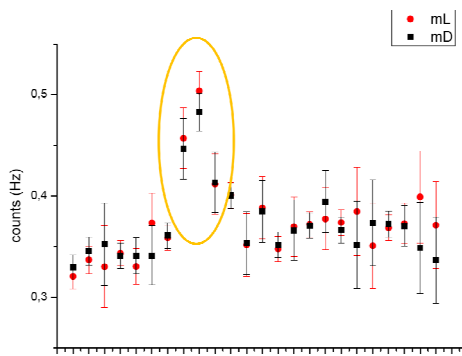


Figure 42: Count rates in the February – March 2008 run. The horizontal axis represents time.

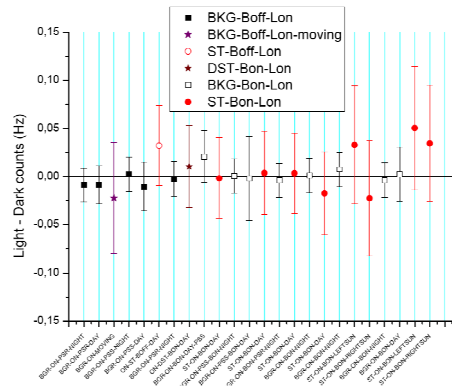


Figure 43: Difference between background and tracking data. The horizontal axis represents time.

In Figure 42 we present the count rates for the February – March 2008 run. “mL” and “mD” labels indicate data taken with the detector either looking at the magnet bore or being blocked by the switch, respectively. The horizontal axis represents time. Data points within the yellow ellipse exhibit a larger count rate, probably ascribable to the first switching on of the magnet or to changes in the room temperature. Data points referring to background or solar tracking data are not plotted together, indicating the fact that no excess of counts is seen when tracking the sun. In Figure 43 each point represents the difference between tracking and background count rates.

Conclusions

The beam tests of the BaRBE setup at CAST showed that is possible to couple a “visible” detector to the magnet bore via an optical fiber without introducing additional background sources with respect to the background measured in the laboratory. The preliminary background rate measured at CAST is

$$\text{DCR} = 0.35 \text{ Hz} \pm 0.02 \text{ Hz}$$

for 30000 s of solar tracking data taking.

In 12 data sets taken during solar tracking (2 sets taken pointing 0.25° degree off-center to the left of the sun and 2 pointing to the right) no excess counts over background were observed.

Two possible ways to improve the detection capability could be foreseen at this stage: 1) a detector with lower dark count rate 2) a resonant cavity inside the magnet bore in order to enhance the axion to photon conversion probability.

Both improvements could be implemented simultaneously, however detailed studies are necessary and compatibility with the CAST apparatus and schedule should be thoroughly checked.

7 CRYOPLANT STATUS

The CAST cryoplant continues to perform extremely well. There have been no significant interruptions to liquid helium production and therefore no interruptions to magnet availability. A major overhaul of the ^4He pumping group has been completed and another major intervention should not be required before 2010. Minor quenches have been initiated on two recent occasions due to external influences: 1) The accidental tripping of a leak detection system in the cryo compressor hall by an external contractor and 2) the accidental discharge of the quench protection system after an electrical perturbation on its supply line. The leak detection system has been clearly marked to avoid a recurrence of the first fault and an interlock and modified procedure will overcome the possibility of a recurrence of the second source of quenches.

One full current quench has also occurred and has been attributed to a natural quench of the magnet, which is to be expected after such a long shut down period.

8 THE SLOW CONTROL STATUS

The CAST Slow Control provides data logging and continuous monitoring. The software is based on National Instrument's LabView7.1. It is composed by two digital data acquisition cards and four analogue data acquisition cards (three with 24-bit resolution and one with 16-bit resolution). The analogue cards are being used to monitor the gas system (pressures, magnet temperature, etc.) and the main parameters of the detectors, while the digital cards are used for the monitoring of the interlock system. In case of interlock alarms or when the pressures or the temperature are out of the normal range, notifications are automatically sent to several CERN GSM and email recipients. During the 2007 upgrading phase many improvements were applied to complete the system (i.e. a residual gas analyser, a laser system for the magnet reference positions) and to allow the monitoring of the ^3He gas system and of the new detectors. The system is connected to an assured power supply to monitor all key experiment parameters also in case of power cut. Moreover a new program connected to a GSM modem allows to determine network problem. The data and status are accessible on-line on a web site to the whole CERN domain and by a remote desktop connection.

9 SUN FILMING

With CAST, it is possible to directly observe the Sun twice a year (March/Sept) through a window in the experimental hall. Thus the tracking system can be tested by an optical crosscheck, the so called “solar filming”. For this purpose, a camera is aligned with the magnet axis and additional software is applied to take into account the refraction of photons in the atmosphere.

During the past, the solar filming has been repeatedly performed successfully. Thus for the data taking phases 2003/04 and 2005/06 it has been confirmed that the magnet was pointing to the Sun with the required accuracy while taking data. Since March 2005, a system with better resolution than the original system used has been working successfully, being able to provide a precision which matches the desired accuracy of the solar tracking (0.02°). It consists of an ST-7 CCD camera and optics with 200 mm focal length.

In order to improve the alignment of this system, it was upgraded in March 2008 by using a laser mounted on a theodolite. The surveyors aligned the laser beam with the theoretical beam axis and by observing the laser with the camera, it could be determined where the magnet is pointing, i.e. where the center of the Sun was expected to be seen.

The data obtained in spring 2008 look promising and analysis is ongoing. First results indicate that the CAST magnet is pointing to the solar core as it was already shown in previous filmings.

Additionally, a new system consisting of a CCD camera and two lasers was used as a complementary method for the sun filming. A schematic is shown in Figure 40. Two diaphragms D1 and D2 are aligned to define a parallel to the magnet beam line axis, with the help of the geometers. The axis is defined with a precision better than 1.7×10^{-5} rad. A laser beam is setup to pass through D1 and D2. A third diaphragm D3 with the second laser, attached on the magnet, allows the magnet positioning with the help of reference marks on the wall. The camera is placed near D1 and is aligned to the theodolite laser. The image of the laser spot ($d=12$ pixels) is the reference for the sun tracking (image of $d=291$ pixels), see Figure 44. Figure 45 shows the image of the sun on the CCD and Figure 46 the remarkable stability of the solar tracking. The results are comparable with the old system and verify the precise alignment of the CAST magnet to the Sun during tracking with a precision of about 1 arcmin.

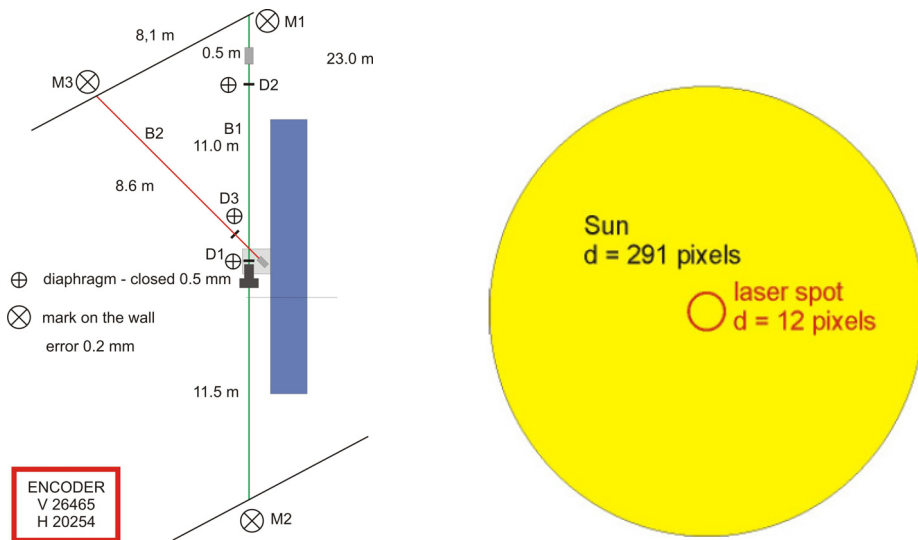


Figure 44: Left: A schematic of the new alignment system. Right: Comparison of the laser spot and the sun image.

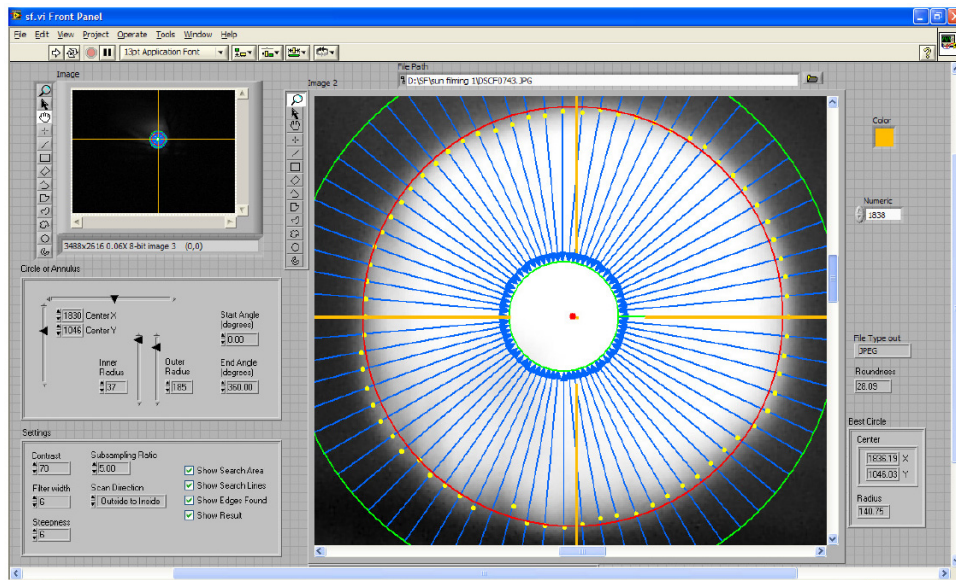


Figure 45: The image of the Sun on the camera CCD.

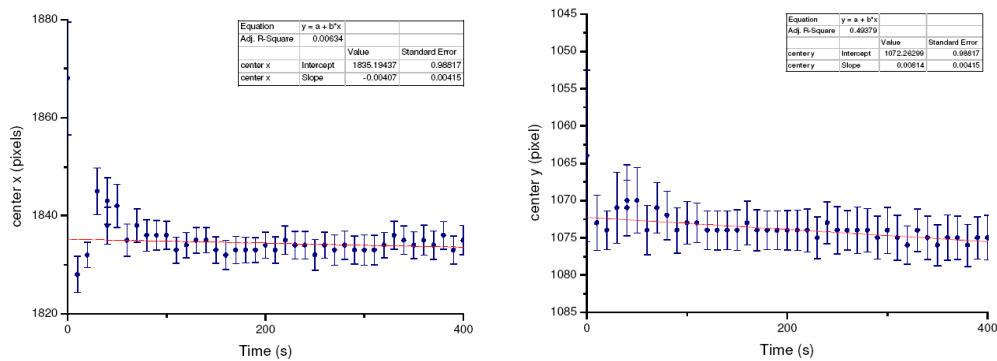


Figure 46: Stability of the x-y solar center coordinates during solar filming.

10 GRID MEASUREMENTS IN 2008

CAST performs periodically the so-called GRID measurements with the help of the team of geometers at CERN. These consist in the independent measurement of the position of the magnet in a set of reference coordinates (GRID) previously defined to cover reasonably all range of movements. These measurements are intended to detect any drift in the pointing ability of the system with respect to the initial calibration values measured in 2002, the ones which are used by the tracking software to determine the real absolute direction in which the magnet is pointing at any time.

The latest measurements were performed during March 2008. The system was found substantially **unchanged** with respect to the October 2007 GRID, and in good agreement with the reference values of the grid of 2002, the ones used for tracking. A small offset of $\sim 1\text{mm}$ at 10 m which is observed in the horizontal direction is well within our acceptance and, furthermore, it can be easily removed by adding an appropriate offset in the horizontal motor encoder.

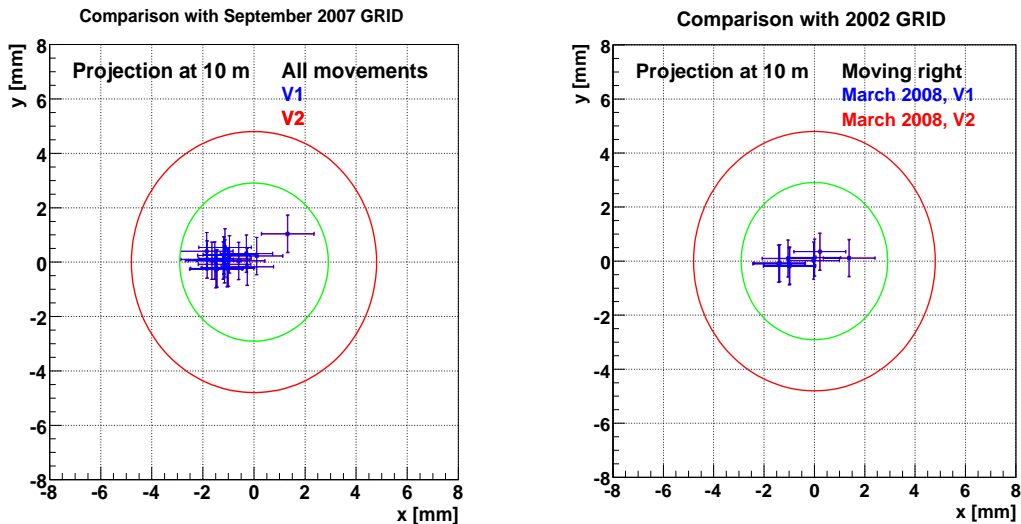


Figure 47: Comparison of March 2008 GRID with the 2007 (left) and 2002 (right) situation. The required precision of 1 arcmin is indicated by the green circle, while the red one represents the 10% of the sun projected at 10 m.

11 CAST EXPERIMENTAL APPARATUS

Magnet movement safety review

Reporting on the proposed safety modifications mentioned in April 2007 SPSC Status Report. All modifications were completed by the summer of 2007. These included:

- Two known weak points on the ‘chariot’ were strengthened.
- The Jura lifting screw had a brass bush inserted at the suspension point to remove gripping on the steel axle.
- The lifting jacks were revised so that they could operate a further 3 years without intervention
- The steel of the main load bearing pivot axles was analysed to confirm the properties were consistent with 16% stronger than those assumed in the safety study.
- A cradle (Figure 48) was installed underneath the magnet at the main pivot in order to restrict any movement of the magnet to 5mm in the event of a failure of the pivot axles.

After the run of 2006, a total of 1.1t was added to the magnet by mid-2007 (^3He system, cradle, MM line and shielding). Due to the replacement of the TPC by smaller MM detectors, the shielding was reduced from 1.1t to 0.5t and the counterweight under the MFB was reduced by 0.6t resulting in the same applied loads at the chariot and the main pivot as in 2006. CAST warmly thanks the TS-MME group for their excellent work in designing and supervising the installation of the safety modifications.

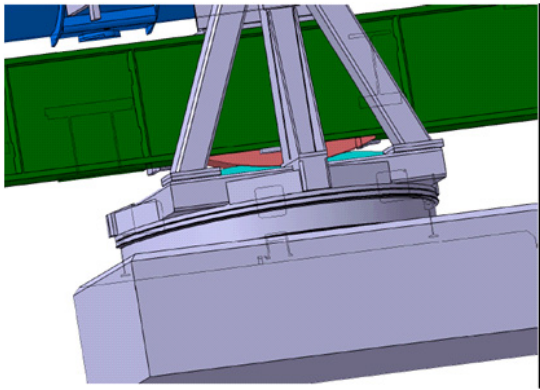


Figure 48a: Safety cradle design



Figure 48b: Safety cradle installed

Magnet power cable support arm – ‘Potence’

During 2007, an inspection of the condition of the magnet power cables was made in view of the known non-ideal conditions of their layout (tight bending radii and frequent movements of the magnet). The experts from FLOHE requested that the tight bending radii at the tip of the Potence be increased to prevent further degradation of the outer rubber hoses (which contain 8 bar circulating cooling water).



Figure 49: Aging of the rubber hoses at tip of Potence



Figure 50: Modifications to the Potence

TS-MME designed and supervised the installation of a mechanical guide on the end of the Potence to increase the bending radii. In addition, a small counterweight was designed to be attached to the Potence to increase the separation between the Potence and the MFB tower to remove an existing problem of close-approach between them. The modified system works well.

The condition of the hoses will be carefully monitored in future and several replacement hoses will be bought as a contingency due to the very long delivery times for new hoses.

12 PHYSICS JUSTIFICATION

Along the lines of the Physics Justification provided in the SPSC 2007 report (CERN-SPSC-2007-012) it is worth adding the following:

CAST phase II with ^3He as buffer gas should cover, at least briefly, every pressure setting that it can achieve (i.e. 1.2 eV) so that we do not miss an unexpectedly strong signal. This implies an appropriate redistribution of the measuring time until the end of 2010. Within the CAST collaboration a discussion and evaluation work is ongoing to definitely fix the running program, i.e. the appropriate pressure setting steps and/or pressure changes per day. However, in order to take the final decision we need to know the definite performance of the three Micromegas detectors. This will be soon the case.

It is worth mentioning that the Tokyo axion helioscope might be already running again, with possible first results later this year. We think however that as long as we are deriving even only limits, the best limits should come from CAST in the axion rest mass range that we can cover. In fact, to compete with Tokyo's results, rather short times per pressure setting would be enough. It is also this aspect which we have to take into account while preparing our short- and longterm schedule.

Concerning the cosmological hot dark matter limit of 1.05 eV as upper limit for the axion rest mass, this is a 95% CL based on the recent WMAP data, not including eventually some systematic errors. One would always want some overlap between the cosmological and laboratory results. Thus, there is some uncertainty, i.e. this is not a hard wall, which justifies our intention to extend the measurements also above this limit. Note also that they only apply to proper QCD inspired axions that couple to pions in the generic way. These limits would NOT apply to general ALPs (Axion Like Particles), which we do not discard as a potential source of a signal, and could be seen with CAST. In fact, as we have argued in our report last year, actually such particles are behind the low energy activity we have already implemented in CAST. In addition, it is worth mentioning that recent theoretical work from a group at DESY on paraphotons refer widely to CAST results, and in particular to the low energy ones which we have not yet published.

13 DETAILS OF RUNNING TIME, COSTS AND RESOURCES REQUIRED FOR 2008 - 2010

i) Running time

The number of calendar days available for sun tracking has been evaluated based on the assumption:

- **2008:** Data taking starting mid week 15 to mid-week 50 except for a 4-week cryo maintenance shutdown in September 2008
- **2009:** Four month shutdown. Cryostat opening (final cold windows, final rupture disk, final instrumentation, vacuum system modifications). Small upgrades to ^3He system e.g. to increase refilling speed. Improvements to external vacuum system, integration of permanent connection ports for low-energy axion detector(s). Final opportunity to install 2nd X-ray optics. Data taking starting week 23 until mid-week 50.
- **2010:** Cryogenic maintenance. Data taking week 14 to week 50.

The running efficiency for the ^3He run 2008-2010 has been re-evaluated recently is based on the following assumptions:

- One change in pressure in the middle of each sun tracking run; morning and then again in the evening
 - Sunset and sunrise detectors measure all pressure settings
 - 72% typical efficiency¹ in taking new pressure settings wrt available calendar days.
 - Axion discovery protocol operating with an average repeat pressure setting fraction of 10%

CAST's aim for the ^3He run was to reach a ^3He density equivalent to 120mbar @ 1.8K by the end of 2010. In view of the reduced total running time now available for the ^3He run of CAST, the nominal pressure step (dP) of typically 0.1 mbar would enable CAST to reach 102 mbar by the end of 2010. An increase of the pressure step by 20% is needed to enable CAST to reach 122 mbar by the end of 2010. The mass coverage for two settings near to 60 mbar @1.8K are shown below for nominal dP (Figure 51) and 1.2dP (Figure 52). Assuming a step of 1.0dP and then 1.2dP, the estimates for the coverage in 2008-2010 are summarised in Table 2 and 3 respectively below.

¹ The 72% efficiency figure is derived from experience gained from taking data in 2006 and from experience gained with the ^3He system after a quench. It takes account also of sun filming, survey grid, X-ray alignment runs and diverse experimental and infrastructure failures. In addition, it contains quenches (6), cold window bake-outs (9) and ^3He refilling time after a quench. The present refilling time of 1mbar/hr is considered too slow for operation above 50 mbar and modifications will be made before the 2009 run to increase the speed of refilling.

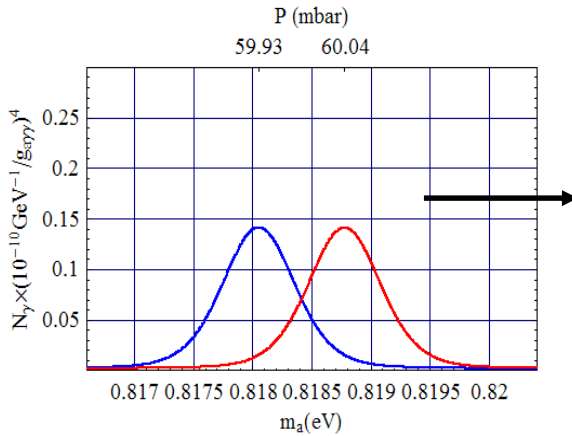


Figure 51a): Mass coverage for two adjacent settings dP =nominal

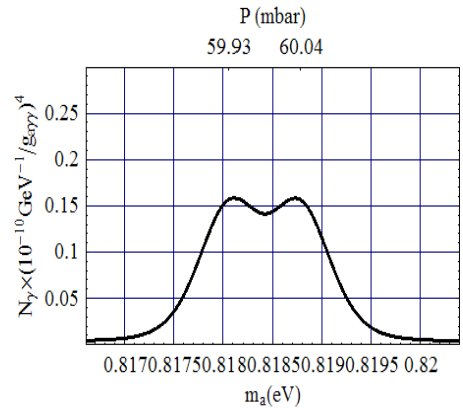


Figure 51b): combined coverage of two settings

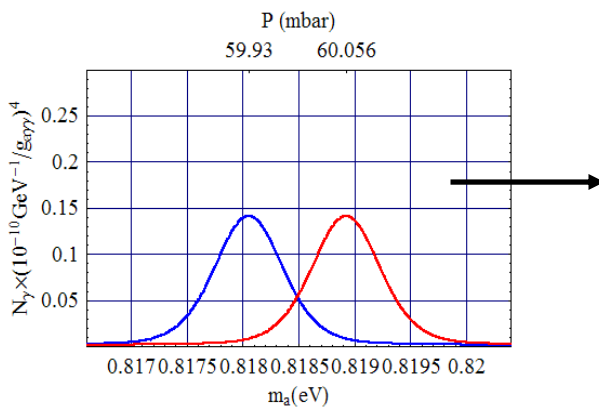


Figure 52a): Mass coverage for two adjacent settings dP =1.2 nominal

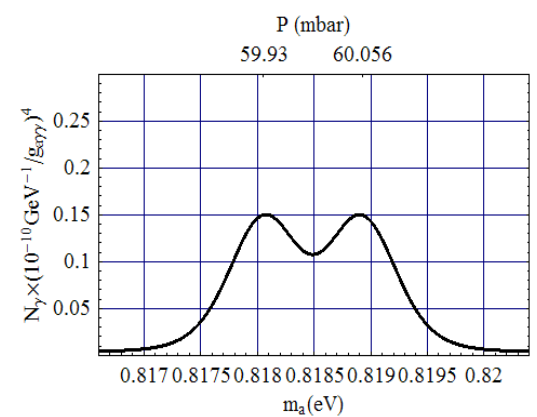


Figure 52b): combined coverage of two settings

The strategy for the CAST data taking remains to execute a continuous ascending pressure scan. Successive small steps are the best way to maximize the discovery potential.

Year	Calendar days	Tracking days including a search protocol (~65%)	Pressure range covered with two settings per tracking (mbar @ 1.8K)
2008	217	144	13.4 - 41 (0.39 - 0.68 eV/c ²)
2009	189	119	41 - 66 (0.68 - 0.86 eV/c ²)
2010	252	162	66 - 102 (0.86 - 1.07 eV/c ²)

Table 2: 2008 to 2010, running time available in calendar days, tracking days after normal losses (including a search protocol), and pressure ranges (with corresponding axion rest mass ranges) achievable each year. The difference between two consecutive pressure settings (the pressure step dP) is calculated with the requirement that the whole mass range is covered equally.

Year	Calendar days	Tracking days including a search protocol (~65%)	Pressure range covered with two settings per tracking (mbar @ 1.8K)
2008	217	144	13.4 - 47 (0.39 – 0.72 eV/c ²)
2009	189	119	47 - 77 (0.72 – 0.93 eV/c ²)
2010	252	162	77 - 122 (0.93 – 1.17 eV/c ²)

Table 3: 2008 to 2010, running time available in calendar days, tracking days after normal losses (including a search protocol), and pressure ranges (with corresponding axion rest mass ranges) achievable each year. In this scenario, the pressure step is slightly increased (1.2 dP)

ii) Costs and resources for CERN

Magnet Running Costs

The costs for CERN as host laboratory of this extension in 2008, 2009 and 2010 for the operation of the magnet are the usual electricity costs for the cryogenics and magnet power converter and the M&O costs of the cryogenic support team, these are shown in Table 4 below.

Item	Dept	Units	2007	2008	2009	2010
Cryogenics M&O (incl gases)	AT	(kCHF)	180	180	180	180
Cryogenics power		(hours)	2976	6720	5500	6720
	TS	(kCHF) ²	82	185	152	185
Magnet Power Supply		(hours)	450	5000	3700	5000
	TS	(kCHF)Err	3	36	26	36
PS Field Support	AB	(kCHF)	3	3	3	3
	CAST	(kCHF)	3	3	3	3
Annual Total		(kCHF)	268	404	361	404
Integrated Total		(kCHF)		404	765	1169

Table 4: Estimates for the cost of running the CAST magnet 2008-2010.

Manpower

CAST is at present experiencing the effects of losing two key personnel (N. Elias - Doctoral Student [³He system] and S. Borghi - Applied Fellow [Slow Control and Run Organisation]) both excellent young physicists and who will both be very difficult to replace. At present CAST does not have a replacement in place and is relying on PhD students from CAST and a shared Fellow with AT-ECR to help bridge the gap until replacements can be found. This situation is a cause of concern.

The CAST collaboration relies on the expert technical support from the Technical Departments at CERN, for which CAST it is very grateful. For the years, 2008-2010, CAST will require continued support from the Technical Departments

² Calculated assuming 55 CHF/MW

at a level similar to that already provided in 2005-2007. The support of the PH Department is essential, as it has been in past years for financial support and manpower to manage and operate CAST and the ^3He system and for technical support for the experiment including the fabrication of the cold X-ray windows. The manpower requests to CERN have been formulated into work packages which are being finalised.

iii) Costs to CAST and Addendum No 3 to the CAST MOU to cover 2008-2010

The funding of the extension for 2008-2010 is detailed in an Addendum No 3 to the CAST MOU which is now available for signing.

An outstanding question, namely the funding for the replacement of the old ABB PLC's in the magnet cryogenics control system by 2 new PLCs has been resolved by the decision to take out a 'hotline' service contract (paid by CAST) with ABB to replace the CERN expert leaving for retirement in 2009.

The funding of the PH CERN CAST contribution is not yet approved.

The Category A budget summary for the years 2008-2010, taken from Addendum No3 to the CAST MOU is shown below in Table 5.

PHASE II ^3He Run	2008	2009	2010	Total
	[kCHF]	[kCHF]	[kCHF]	[kCHF]
General M&O				
Personnel	185	148	129	462
Experimental operation costs	174	179	174	527
Cryogenic ABB contract	0	25	25	50
Sub-total	359	352	328	1039
Investments in Common Items				
Investments in instrumentation and infrastructure	147	116	49	312
Investments in Detector Construction & Infrastructure	40	30	20	90
Sub-total	187	146	69	402
Grand Total	545	498	397	1441
Presently expected Contributions	477	424	409	1311
Present balance³				-130

Table 5: Budget summary for Category A costs 2008-2010.

Due to the shortage of personnel at CERN, the personnel component of the General M&O budget has had to be increased significantly compared with the cost estimates in the 2007 status report. This is to fund visiting physicists to participate in the running and to share the responsibilities in Slow Control and parts of the ^3He system. In addition, the Experimental operation costs are more realistic and now contain contingencies for increased working space, soundproofing work in CAST and around the LHCb power converter, new rubber hoses for the magnet power cables and strategic spares for the ^3He system.

The estimates for the expenditure in the collaborating institutes for detector consolidation and investment (Category B) costs are now 455kCHF for X-ray detectors and 159kCHF for Low Energy detector development.

At present there are 20 Institutes preparing to sign the Addendum No3 represented by 47 PhD physicists.

³ Additional contributions are being requested to cover the present shortfall. Any deficit that finally remains will have to be addressed by curtailing the run in 2010

14 CONCLUSIONS

In conclusion, CAST has derived already the best laboratory results for axion masses up to 0.39 eV, apart for the range from about 10^{-6} – 10^{-5} eV being covered by dark matter experiments. The CAST results surpass or at least compete in an axion rest mass range up to ~ 0.02 eV the best astrophysically obtained limits for the axion-to-photon coupling constant. In the already scanned mass range from 0.02 eV up to ~ 0.39 eV the derived limits are worse than the astrophysical limits, but they are the best laboratory values. CAST is moving towards the theoretically motivated parameter phase space, which overlaps also with the astrophysical limits, and has the potential to even surpass the most conservative rest mass limit of about 1.05eV as it has been derived from cosmology, i.e. from WMAP data.

CAST has just embarked on the first data taking of the ^3He run of Phase II. The transition to ^3He running has taken longer than foreseen despite a huge effort on behalf of the CAST personnel involved. The running program can be tailored to compensate for the loss in running time by increasing the pressure step size by 20%.

There has also been a large effort in the detector field; firstly to recover a potentially serious problem which arose in the CCD. The CCD detector is now again functioning as before and the telescope has had a successful mid-term test at PANTER removing any questions of degradation in performance in the CAST experimental conditions. Secondly, the Micromegas (MM) team have made large progress towards equipping the three remaining lines with more competitive, shielded detectors. At present two MMs are considered fully operational a third only partially operational (which will be changed when a suitable occasion arises). These detectors will be used to either enhance the CAST sensitivity provided by the CCD or provide an adequate sensitivity in case of any temporary absence of CCD data.

Furthermore, motivated by various longstanding solar observations of as yet unknown origin which happens to take place predominantly in the sub-keV range, and, along with the widely discussed axion-like particles in the literature, CAST has entered since November 2007 into the low energy domain. In fact, CAST has performed since November 2007 two solar tracking periods of one week each, in the few eV range (the so called "visible run"). This is already a novel item in solar axion physics, since the impact of the previously ignored magnetic fields in solar modelling might show-up as axion-like signatures in such searches. More such measurements are considered and without interfering with the base program. In addition, if all 4 CAST detectors perform optimally, the collaboration will discuss the option to follow more actively the low energy search.

The Collaboration has new members and an evolving Low Energy axion physics and detector development program, where a permanent setup for this application will be designed in 2008 for integration in early 2009.

CAST is now ready to reap the fruits of the heavy investment and hard work of 2007 being now equipped with a flexible and high-performance ^3He system and with beam lines supplied with detectors of enhanced sensitivity. CAST results have an impact in the international astroparticle physics community. The CAST experiment has significantly contributed to the development of the proper techniques to understand the nature of the axions and has inspired new theoretical and experimental work on the search and possible discovery of these illusive particles. The renovated detector setup and the ^3He system will explore further uncharted but promising regions of phase space.